Electron-ion energy partition when a charged particle slows in a plasma: Theory

Lowell S. Brown, Dean L. Preston, and Robert L. Singleton Jr. Los Alamos National Laboratory Los Alamos, New Mexico 87545, USA (Received 12 April 2012; published 23 July 2012)

The preceding paper [Brown, Preston, and Singleton Jr., Phys. Rev. E 86, 016406 (2012)] presented precise results for the partition of the initial energy E_0 of a fast particle into the ions and electrons— E_1/E_0 and E_e/E_0 —when the fast particle slows in a plasma whose ion and electron temperatures may differ. As emphasized in that paper, this is an important problem because nuclear fusion reactions, such as those that occur in an inertial confinement fusion capsule, involve ion temperatures that run away from the electron temperatures. As also noted in the preceding paper, a precise evaluation entails the use of a well-defined Fokker-Planck equation for the phase-space evolution of initially fast projectile particles. When the plasma has differing ion and electron temperatures, the projectiles must slow into a "schizophrenic" final ensemble of particles that has neither the electron nor the ion temperature. This is not a simple Maxwell-Boltzmann distribution since the electrons are not in thermal equilibrium with the ions. Thus, detailed calculations are required for the solution of the problem. These we provide here for a weakly to moderately coupled plasma. The Fokker-Planck equation holds to first subleading order in the dimensionless plasma coupling constant, which translates to computing to order $n \ln n$ (leading) and n (subleading) in the plasma density n. The energy partitions for a background plasma in thermal equilibrium have been previously computed, but the order n terms have not been calculated, only estimated. The "schizophrenic" final ensemble of slowed particles gives a new mechanism to bring the electron and ion temperatures together. The rate at which this new mechanism brings the electrons and ions in the plasma into thermal equilibrium will be computed.

DOI: 10.1103/PhysRevE.86.016407 PACS number(s): 52.20.-j, 52.25.Dg, 52.57.-z

I. INTRODUCTION

The underlying theme of this paper is the thermonuclear burn of deuterium-tritium plasmas. We do not consider the initiation of the burn process, which is system specific, nor are we interested in the late stages of the process when most of the deuterium-tritium (DT) fuel has been burned into α particles and neutrons, and the electrons and ions are nearly in thermal equilibrium. We instead focus on intermediate times when, in general, there is a significant difference between the electron and ion temperatures, but the α particle density has not yet become a significant fraction of the D and T ion densities.¹ The fusion rate is very sensitive to the ion temperature T_1 . The ion temperature is determined by competition between deposition of the α -particle energy into the ions, which, of course, increases T_1 , and thermal equilibration with the electron distribution, which drives T_1 down. Our main concern in this paper is the partition of the total α energy between the ions and electrons in a two-temperature plasma in the circumstances that we have outlined.² This is important in the understanding of the time scale and the robustness of the fusion process. Our evaluations of the functions which determine the energy partition do not include a contribution from the α particles; hence, our results are valid only if the ensemble of αs is sufficiently dilute. We find that the α particles slow down into

terms in the energy partition, we have computed exactly the

coefficient of the order n term, which has previously been only

estimated. We turn now to describe our work in some detail.

a non-Maxwellian distribution in which the mean α energy \bar{E} lies between the thermal energies of the ions and electrons. Our

work shows that these nonthermal α particles increase the rate

of energy transfer between the electrons and ions but, since we

do not examine late times when the population of α particles is

large, this new mechanism does not significantly enhance the

energy transfer rate. In general, as in other work on stopping

power and the partition of a fast projectile particle's energy

between the electrons and ions in the plasma, we assume

(as is most often the case) that the stopping times are much

shorter than the time scale of the fusion so we can work in

the adiabatic approximation in which the time dependencies

of our results are only those brought about by the changes in

the plasma parameters on which they depend. We also require,

as is generally assumed, that the charged particle range is

016407-1

short in comparison with the distances over which the plasma conditions vary so the plasma may be treated as uniform. The purpose of this paper is to provide the detailed theoretical description of the energy transfer to the electrons and ions in the plasma when a fast particle slows—to provide the theoretical basis for the results described in the preceding paper [2]. Using our theory, we have worked out the energy partition for differing electron and ion temperatures; this has not been previously considered in the literature. Second, even for the case of equal ion and electron temperatures, where the α s relax into a Maxwellian distribution, we have made two improvements. We have developed a formulation that precisely defines the energy partition so a correction of order T/E_0 is now included, a correction that is missing in the literature. In addition to the well-known $n \ln n$ (n is the number density)

¹When the α particle density is a significant fraction of the plasma ion density, the effect of the α s on the dielectric response of the plasma must be taken into account. This introduces additional complications and, as such, merits a separate publication.

²A short preliminary account of the methods that we employ in this paper, but restricted to the case of equal ion and electron temperatures, has previously been presented in Ref. [1].

In our work, we do not follow the trajectory of a single projectile particle. Rather, we achieve a much simpler theoretical framework by considering a time-independent situation in which initial projectile (impurity) particles are continuously created and slow into a nonthermal distribution. This is akin to examining the steady motion of a fluid rather than the much more complicated motion of a single atom. The problem is further simplified by assuming that the sources of the charged projectile particles (the α particles in DT fusion) are uniformly distributed throughout the plasma and that the initial energetic particles are created with an isotropic velocity distribution; hence, the phase-space distribution of the projectile particles is only a function of the energy and time. The evolution of this distribution is governed by a Fokker-Planck equation derived³ by Brown, Preston, and Singleton (BPS) [3]. After first establishing the proper conditions, which does involve an initial time evolution, but one that is easily treated with the proper formalism, we then pass to a time-independent, steady state, so we need solve only ordinary differential equations in the projectile particle's energy.

The Fokker-Planck equation involves coefficient functions $\mathcal{A}_{I}(E)$ and $\mathcal{A}_{e}(E)$ which were computed in BPS to order $n(\ln n + c)$ in the plasma density n. Their definition is rather complicated; hence, it is deferred to Appendix A, which presents a detailed description. Since $n \sim g^2$, with g the plasma coupling constant, it is evident that these two terms in the density are the leading and first subleading terms in the perturbative expansions in g of the coefficient functions. Higher-order terms in the expansions become significant at high densities; hence, our results are not applicable, in particular, to (strongly coupled) warm dense plasmas. Numerical simulations provide the only potentially reliable means of validating our analytic expressions for the energy partition extended to moderately coupled plasmas and for evaluating the partition in the strongly coupled case. Although such computations have not been performed, careful, large statistics, molecular dynamics (MD) simulations have been carried out by Dimonte and Daligault [5] to investigate a different process, the electron-ion temperature relaxation. They have done so over a wide range of plasma parameters that span weak to strong coupling. Their MD results for the Coulomb logarithm for this process agree with those of BPS [3] for g < 0.2 to within the statistical uncertainty of $\pm 5\%$ in the simulations, with a difference of about 15% for g = 0.3 that grows rapidly for g > 0.3. This indicates the range of validity of the Fokker-Planck equation that we use to compute a different process, the energy partition.

Following a detailed discussion of the Fokker-Planck equation in Secs. II A and II B, the late-time distribution $f_{\infty}(E)$ of a $\delta(t)$ source of projectile (impurity) particles, which is needed to obtain the electron-ion energy split, is derived in Sec. II C. In Sec. III a source is slowly turned on and eventually emits particles at a constant rate. The solution f(E,t) of

the now inhomogeneous Fokker-Planck equation is shown to be the sum of two terms: $f(E,t) = n(t) f_{\infty}(E) + \bar{f}(E)$, where n(t) is the number density of projectile particles that have come into the distribution described by $f_{\infty}(E)$, and $\bar{f}(E)$, which describes the transfer of energy to the electrons and ions. The energy losses E_e and E_1 to the electrons and ions are expressed as single integrals involving the function $\bar{f}(E)$ [whose computation involves the \mathcal{A} coefficients] and the \mathcal{A} coefficients themselves. For differing electron and ion temperatures, the late-time energy distribution $f_{\infty}(E)$ of the projectile particles is not a Maxwell-Boltzmann distribution. This ensemble increases the rate of ion-electron thermal equilibration above that of the impurity-free plasma. In Sec. IV A we carry out the explicit construction of $\bar{f}(E)$.

We, first, discuss our precise results for equal ion and electron temperatures in Sec. IV B and then go on in Sec. IV C to compute E_1/E_0 and E_e/E_0 for the general case of different plasma electron and ion temperatures in terms of integrals over A_1 and A_e . At this point, as summarized in Sec. V, we have finished a logically complete exposition of our methodology and results, which is essentially self-contained. However, for those interested in supporting details and who may wish to work out the intermediate steps in our calculations, we include these details in the appendices. We provide a review of the Afunctions that were computed in BPS [3] which are needed for the present work in Appendix A, a host of details on these functions that include their approximate forms in various regions in Appendix B, and an accurate approximation for one of the two multiple integrals appearing in our final expressions for E_1 and E_e is provided in Appendix C.

II. FORMULATION OF THE PROBLEM

A. The Fokker-Planck equation to leading and next-to-leading order

We consider a plasma containing a dilute population of projectile particles with a phase-space density $f(\mathbf{r},\mathbf{p},t)$. For example, in a DT plasma, the impurities could consist of the charged α particles produced from the DT fusion. The problem we shall address is the manner by which such impurities reach the $f_{\infty}(E)$ distribution. During this process, the impurities deposit portions of their energy to plasma electrons and plasma ions, and the formalism we now develop will allow us to compute the electron-ion energy splitting in a systematic and unambiguous fashion. We take the plasma to have an electron temperature $T_e = \beta_e^{-1}$ and a common temperature $T_i = \beta_i^{-1}$ for all the ions, in which case the Fokker-Planck equation for the distribution f of an projectile species has the form

$$\left[\frac{\partial}{\partial t} + \mathbf{v} \cdot \nabla\right] f(\mathbf{r}, \mathbf{p}, t)
= \sum_{b} \frac{\partial}{\partial p^{k}} C_{b}^{k\ell}(\mathbf{p}) \left[\beta_{b} v^{\ell} + \frac{\partial}{\partial p^{\ell}}\right] f(\mathbf{r}, \mathbf{p}, t), \quad (2.1)$$

where $\mathbf{v} = \mathbf{p}/m$ is the velocity of a projectile particle with momentum \mathbf{p} , the explicit sum runs over all the particle species b in the background plasma, and the summation convention is used for repeated vector indices k and ℓ . As we shall describe more fully, the diffusion coefficient $C_b^{k\ell}$ has been analytically calculated to leading and next-to-leading orders

³This derivation utilizes a rather subtle method of dimensional continuation. Although we shall make no use of the dimensional continuation method in this paper, we note that a detailed, pedagogical explanation of the method that facilitates the understanding of the results derived in BPS [3] is contained in Secs. IV and V in Ref. [4].

in the plasma density in BPS [3] or, more precisely, to orders $g^2 \ln g^2$ and g^2 in the generic dimensionless plasma coupling constant $g = e^2 \kappa / 4\pi T$. We use rationalized electrostatic units, so this parameter is the Coulomb energy of two particles of charge e a Debye distance $1/\kappa$ apart divided by an average temperature T.

With our conventions, the number of projectile particles is given by

$$N(t) = \int d^3r \int \frac{d^3p}{(2\pi\hbar)^3} f(\mathbf{r}, \mathbf{p}, t), \qquad (2.2)$$

and their kinetic energy appears as

$$E(t) = \int d^3r \int \frac{d^3p}{(2\pi\hbar)^3} \frac{p^2}{2m} f(\mathbf{r}, \mathbf{p}, t).$$
 (2.3)

Here we normalize phase-space integration measures with the factors $(2\pi\hbar)^3 = h^3$ in the denominators. We do this because h is the phase-space volume of one quantum state. Since the right-hand side of the Fokker-Planck equation (2.1) contains an overall total momentum derivative, it does not contribute to the time rate of change of the particle number—the Coulomb collisions in the plasma preserve particle number. When the electrons and ions are at common temperature $T = \beta^{-1}$, the terms in the final square brackets in the Fokker-Planck equation (2.1) annihilate a thermal Maxwell-Boltzmann distribution $[f \propto \exp\{-\beta \mathbf{p}^2/2m\}]$ of projectile particles—a collection of particles in thermal equilibrium is not altered by their collisions with a background plasma at the same temperature. However, for those cases in which the ions and electrons have different temperatures, the projectile particles attain a nonthermal quasistatic distribution that will be described shortly. Eventually this quasistatic distribution will relax into a thermal distribution as the electron and ion components themselves thermally relax. As we shall see, however, the projectile distribution has interesting effects on temperature relaxation at intermediate times.

The stopping power can be extracted from the Fokker-Planck equation by considering a single projectile particle at \mathbf{r}_p moving with the velocity \mathbf{v}_p . The corresponding distribution function is given by $f_p(\mathbf{r}, \mathbf{p}, t) = (2\pi\hbar)^3 \delta(\mathbf{r} - \mathbf{r}_p)\delta(\mathbf{p} - \mathbf{p}_p)$, and one can easily check that this distribution indeed gives N=1 as it should. Inserting this single-particle distribution into Eq. (2.1) and performing a partial integration, it is easy to see that the rate of energy loss of the particle is given by

$$\frac{dE}{dt} = +\sum_{b} \left(\beta_b v_p^{\ell} - \frac{\partial}{\partial p_p^{\ell}} \right) v_p^{k} C_b^{k\ell}(\mathbf{p}_p). \tag{2.4}$$

To make the sign of this expression clear, we emphasize that it gives the rate at which the particle *loses* energy to the plasma [it is the negative of the time derivative of Eq. (2.3)]. Hence, the stopping power, which is the energy loss of the particle per

$$\exp[\mu/T - (1/2)mv^2/T],$$

in which μ is the chemical potential.

unit distance traveled, appears as

$$\frac{dE}{dx} = +\frac{1}{v_n} \frac{dE}{dt}.$$
 (2.5)

B. Longitudinal and transverse components of the diffusion tensor

As described in detail in BPS, the isotropy of the background thermal plasma allows one to decompose the diffusion tensor as

$$C_b^{k\ell}(\mathbf{p}) = \mathcal{A}_b(v) \frac{\hat{v}^k \hat{v}^\ell}{\beta_b v} + \mathcal{B}_b(v) \frac{1}{2} \left(\delta^{k\ell} - \hat{v}^k \hat{v}^\ell\right), \quad (2.6)$$

where v is the magnitude of the velocity, $v = |\mathbf{v}|$, with the velocity direction given by $\hat{\mathbf{v}} = \mathbf{v}/v$. We often take the independent variable to be the energy $E = \frac{1}{2} m v^2$ and, with a slight abuse of notation, we shall also write $\mathcal{A}_b = \mathcal{A}_b(E)$ and $\mathcal{B}_b = \mathcal{B}_b(E)$. As a matter of completeness, the \mathcal{A} coefficients are provided in Appendix A, and their various limits can be found in Appendix B. For a homogeneous and isotropic source of projectile particles, the case we shall consider, the \mathcal{B} coefficients do not enter, although their analytic forms can be found in BPS [3] if desired.

Let us return to the stopping power (2.4) of a charged particle. Since the velocity tensor multiplying the \mathcal{B} contribution is transverse—its contraction with v^k or v^ℓ vanishes—the rate of energy loss (2.4) of a projectile becomes

$$\frac{dE}{dt} = \sum_{b} \left(v - \frac{1}{\beta_{b}m} \frac{\partial}{\partial v^{\ell}} \hat{v}^{\ell} \right) \mathcal{A}_{b}, \tag{2.7}$$

where we have now omitted the p subscript. The respective energy losses to the ions and electrons are given by separating this formula into the ion contribution described by

$$A_{\rm I} = \sum_{i} A_{i}, \qquad (2.8)$$

and the electron part governed by A_e , so⁵

$$\frac{dE_{\rm I}}{dt} = \left(v - \frac{1}{\beta_{\rm I}m} \frac{\partial}{\partial v^{\ell}} \hat{v}^{\ell}\right) \mathcal{A}_{\rm I} \tag{2.9}$$

⁵As noted in BPS, to the order in g in which we are working, namely to leading $(g^2 \ln g^2)$ and next-to-leading (g^2) order, only the kinetic energy of the stopping ion enters, and a meaningfully separation into electron and ion energy components can be made. This is because of the trivial fact that the kinetic energy is independent of g-it is of order g^0 . In addition to this kinetic energy, the projectile particle has potential energy interactions with the ions in the background plasma. The change in these interaction energies associated with the motion of an projectile particle in a plasma cannot be separated into different parts that are associated with the ions and with the electrons. This is because this potential energy starts out at order g, and, thus, its evolution, which involves interactions akin to those involved in the kinetic energy dE/dx, is of order g^3 (modulo possible logarithms), an order that is higher than that considered in this paper. Thus, it should be emphasized that at higher orders in g, such clean separation into energies deposited into well-defined, separate ion and electron components cannot be performed.

⁴With this normalization, the Maxwell-Boltzmann distribution for each spin state of a particle is simply

and

$$\frac{dE_e}{dt} = \left(v - \frac{1}{\beta_e m} \frac{\partial}{\partial v^\ell} \hat{v}^\ell\right) \mathcal{A}_e, \tag{2.10}$$

with their sum giving

$$\frac{dE}{dt} = \frac{dE_{\rm I}}{dt} + \frac{dE_e}{dt}.$$
 (2.11)

In particular, we should emphasize that our Fokker-Planck equation describes a particle's energy loss, including orders $g^2 \ln g^2$ and g^2 with no ambiguity.⁶

Rather than tracking an individual charged particle slowing down in the plasma, it is much simpler—and equivalent—to examine an isotropic distribution of particles. When the projectile particle distribution is isotropic, f is a function the magnitude of the momentum $p = |\mathbf{p}|$ or, equivalently, of the speed v or energy E. In such cases, a momentum derivative of f produces a factor of the velocity vector whose contraction with the velocity tensor multiplying the \mathcal{B}_b coefficients vanishes. Hence, in the isotropic case, the Fokker-Planck equation (2.1) reduces to

$$\left[\frac{\partial}{\partial t} - \frac{\partial}{\partial \mathbf{v}} \cdot \hat{\mathbf{v}} \sum_{b} \frac{\mathcal{A}_{b}}{m} \left(1 + \frac{\hat{\mathbf{v}}}{\beta_{b} m v} \cdot \frac{\partial}{\partial \mathbf{v}}\right)\right] f(E, t) = 0.$$
(2.12)

To avoid notational clutter, we define the total ${\cal A}$ coefficient by

$$\mathcal{A}(E) = \mathcal{A}_{I}(E) + \mathcal{A}_{e}(E), \qquad (2.13)$$

and the temperature-weighted A coefficient by

$$\langle T \mathcal{A}(E) \rangle = T_{\rm I} \mathcal{A}_{\rm I}(E) + T_{e} \mathcal{A}_{e}(E).$$
 (2.14)

Thus.

$$\left\{ \frac{\partial}{\partial t} - \frac{\partial}{\partial \mathbf{v}} \cdot \hat{\mathbf{v}} \left[\frac{\mathcal{A}(E)}{m} + \frac{\langle T \mathcal{A}(E) \rangle}{m^2 v} \hat{\mathbf{v}} \cdot \frac{\partial}{\partial \mathbf{v}} \right] \right\} f(E, t) = 0.$$
(2.15)

Using the operator forms

$$\frac{\partial}{\partial \mathbf{v}} \cdot \hat{\mathbf{v}} = v^{-2} \frac{\partial}{\partial v} v^2 = \frac{2}{v} \frac{\partial}{\partial E} E \tag{2.16}$$

and

$$\hat{\mathbf{v}} \cdot \frac{\partial}{\partial \mathbf{v}} = \frac{\partial}{\partial v} = mv \frac{\partial}{\partial E}, \tag{2.17}$$

we may express Eq. (2.15) in the form

$$\left\{ \frac{\partial}{\partial t} - \frac{2}{mv} \frac{\partial}{\partial E} E \left[\mathcal{A}(E) + \langle T \mathcal{A}(E) \rangle \frac{\partial}{\partial E} \right] \right\} f(E,t) = 0.$$
(2.18)

C. Asymptotic solution

As we shall see, to use these results to obtain an unambiguous formulation of the fractions of the total energy deposited into the ions and electrons, we, first, need to compute the asymptotic distribution into which an initial swarm of projectile particles relaxes in the presence of a background plasma of differing electron and ion temperatures. This quasistatic distribution will be a function of E (or equivalently of p), which we express in terms of a function S(E) as

$$f_{\infty}(E) = \mathcal{N} e^{-S(E)}, \tag{2.19}$$

where we choose N to normalize the distribution to unity,

$$1 = \mathcal{N} \int \frac{d^3 p}{(2\pi\hbar)^3} e^{-S(E)}.$$
 (2.20)

The function S(E) is determined by inserting the structure (2.19) into Eq. (2.18) which gives

$$\frac{d}{dE} E \left[\mathcal{A}(E) + \langle T \mathcal{A}(E) \rangle \frac{d}{dE} \right] e^{-S(E)} = 0. \quad (2.21)$$

One solution of the second-order differential equation (2.21) is obtained by requiring that the quantity in square brackets operating on $\exp\{-S(E)\}$ vanishes:

$$\mathcal{A}(E) - \langle T \mathcal{A}(E) \rangle \frac{dS(E)}{dE} = 0,$$
 (2.22)

and the solution can be obtained by a simple integration,

$$S(E; T_e, T_1) = \int_0^E dE' \frac{\mathcal{A}(E')}{\langle T \mathcal{A}(E') \rangle}.$$
 (2.23)

Here we have temporarily indicated the explicit dependence on the electron and ion temperatures to emphasize that when the ions and electrons are at a common temperature $T = T_1 = T_e$, this solution reduces to the Maxwell-Boltzmann distribution

$$S(E;T,T) = \frac{E}{T},\tag{2.24}$$

and, consequently, a swarm of projectile particles simply relaxes to the background plasma equilibrium distribution. For the equal temperature solution (2.24), a simple analytic Gaussian integration evaluates the normalization factor defined in Eq. (2.20) as

$$\mathcal{N} = \left(\frac{2\pi\hbar^2}{mT}\right)^{3/2}.\tag{2.25}$$

Expression (2.23) is indeed the physical solution for S(E). This is because, having the solution (2.23) in hand, it is a matter of simple quadratures to construct the second, linearly independent solution for our second-order differential equation (2.21). It is not difficult to then confirm that this second solution is not normalizable, and so our first solution is the only physically relevant solution. We can also see that this is the desired solution since, for equal temperatures, it relaxes to a thermal Maxwellian distribution.

The Maxwell-Boltzmann distribution has an average energy of 3T/2. However, for the ions and electrons at different

⁶See BPS [3] for a full discussion of the range of validity of the Fokker-Planck equation.

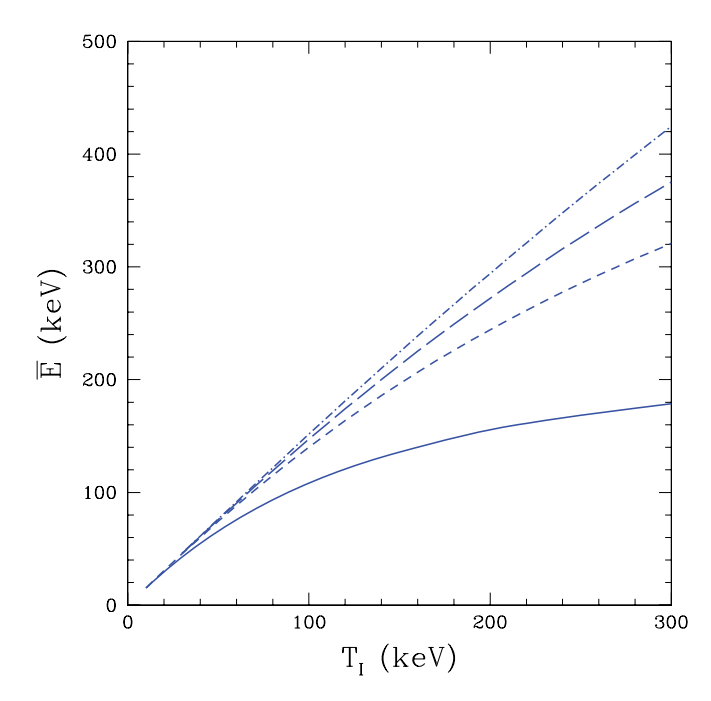


FIG. 1. (Color online) Average energy \bar{E} to which the α particle relaxes as a function of the ion temperature $T_{\rm I}$ for various electron temperatures T_e . The ascending curves describing larger values of \bar{E} have the increasing electron temperatures $T_e=10$, 30, 50, 100 keV (solid, short-dashed, long-dashed, dot-dashed). When $T_e=T_{\rm I}=T$ then $\bar{E}=\frac{3}{2}T$. The background plasma is equimolar DT with electron number density $n_e=1.0\times 10^{25}~{\rm cm}^{-3}$.

temperatures, the swarm of projectile particles relaxes to the average energy

$$\bar{E} = \mathcal{N} \int \frac{d^3 \mathbf{p}}{(2\pi\hbar)^3} \frac{p^2}{2m} \exp \left[-S \left(\frac{p^2}{2m} \right) \right]. \tag{2.26}$$

In this case, numerical integrations are needed to evaluate the normalization constant \mathcal{N} and the average energy \bar{E} . Figure 1 plots the average final energy \bar{E} for an α particle in an equimolar DT plasma with an electron density $n_e = 1.0 \times 10^{25} \text{ cm}^{-3}$. The figure displays \bar{E} as a function of the ion temperature $T_{\rm I}$ for various electron temperatures T_e .

III. FORMAL SOLUTION

A. A homogeneous and isotropic source

We shall assume that the background plasma parameters, such as its density and temperatures, change very little over distances that are large in comparison with the stopping distance of the charged projectile particles and that the plasma parameters also change very little during the stopping time. Thus, the plasma is treated as homogeneous and static. In addition, we assume that the sources of the projectile particles are distributed uniformly in space and that they emit the projectile particles isotropically with a definite energy E_0 . For example, the fusion process in a homogeneous DT plasma produces α particles uniformly in space and isotropically in angle with an initial energy of $E_0 = 3.54$ MeV. Thus, instead of considering the motion of a single projectile particle, we compute energy partitions and final states of charged

particles emitted isotropically with a definite energy E_0 from a uniform distribution of sources. This greatly simplifies the problem in that we can employ the homogeneous Fokker-Planck Eq. (2.18) except that it is now modified to include a time-varying source of particles of energy E_0 :

$$\left\{ \frac{\partial}{\partial t} - \frac{2}{mv} \frac{\partial}{\partial E} E \left[\mathcal{A}(E) + \langle T \mathcal{A}(E) \rangle \frac{\partial}{\partial E} \right] \right\} f(E,t) \\
= \delta \left(E - E_0 \right) s(t). \tag{3.1}$$

The number and energy densities, n(t) and $\mathcal{E}(t)$, are simply given by removing the spatial volume integrations from the previous definitions (2.2) and (2.3). The inhomogeneous Fokker-Planck equation (3.1) gives the time variations of these quantities:

$$\dot{n}(t) = \int \frac{d^3 \mathbf{p}}{(2\pi\hbar)^3} \,\delta\left(E - E_0\right) \, s(t) = \frac{s(t)}{2\pi^2\hbar^3} \,\sqrt{2m^3 E_0} \quad (3.2)$$

and

$$\dot{\mathcal{E}}(t) = E_0 \dot{n}(t) - \int \frac{d^3 \mathbf{p}}{(2\pi\hbar)^3} v \left\{ \left[\mathcal{A}_{\mathsf{I}}(E) + \mathcal{A}_{e}(E) \right] + \left[T_{\mathsf{I}} \mathcal{A}_{\mathsf{I}}(E) + T_{e} \mathcal{A}_{e}(E) \right] \frac{\partial}{\partial E} \right\} f(E, t). \tag{3.3}$$

When the projectile particle source s(t) is turned on and then attains a constant fixed value s_0 , the number density n(t) eventually increases linearly in time,

$$n(t) = \int_{-\infty}^{t} dt' \, \dot{n}(t') = \frac{\sqrt{2m^3 E_0}}{2\pi^2 \hbar^3} \int_{-\infty}^{t} dt' \, s(t')$$
$$= \dot{n}_{\infty} t + \text{constant}, \tag{3.4}$$

where

$$\dot{n}_{\infty} = \frac{s_0}{2\pi^2 \hbar^3} \sqrt{2m^3 E_0}.$$
 (3.5)

B. Asymptotic solution to the inhomogeneous problem

We turn now to obtain the asymptotic solution to (3.1) satisfying the initial condition that there are no projectile particles in the distant past.

As a first step in obtaining the asymptotic solution of the inhomogeneous Fokker-Planck equation (3.1), we set

$$f(E,t) = \exp[-S(E)/2] g(E,t).$$
 (3.6)

Multiplying the resulting Fokker-Planck equation by $\exp[S(E)/2]$ on the left yields a similarity transformation that converts the (velocity \sim momentum) differential operator structure in Eq. (3.1) into

$$H = -\left[\frac{\partial}{\partial \mathbf{p}} \cdot \hat{\mathbf{v}} - \frac{v\mathcal{A}(E)}{2\langle T\mathcal{A}(E)\rangle}\right] \frac{\langle T\mathcal{A}(E)\rangle}{v}$$
$$\times \left[\hat{\mathbf{v}} \cdot \frac{\partial}{\partial \mathbf{p}} + \frac{v\mathcal{A}(E)}{2\langle T\mathcal{A}(E)\rangle}\right], \tag{3.7}$$

so the new Fokker-Planck equation now appears as

$$\left(\frac{\partial}{\partial t} + H\right) g(E, t) = \delta \left(E - E_0\right) e^{S(E_0)/2} s(t). \tag{3.8}$$

Incorporating the boundary condition that the solution vanishes initially, the inhomogeneous differential equation (3.8) has a formal solution:

$$g(E,t) = \int_{-\infty}^{t} dt' \, e^{-H(t-t')} \, \delta\left(E - E_0\right) \, e^{S(E_0)/2} \, s(t'). \tag{3.9}$$

Because of the operator nature of the formal solution (3.9), it is convenient to view functions in momentum space as vectors in an abstract real vector space and define an inner product by

$$(\psi, \chi) = \int \frac{d^3 \mathbf{p}}{(2\pi\hbar)^3} \, \psi(\mathbf{p}) \, \chi(\mathbf{p}). \tag{3.10}$$

With obvious partial integrations, it is straightforward to verify that H considered as an operator on this function space is Hermitian with this definition of the inner product.

In view of our previous work, it is easy to check that

$$\phi(\mathbf{p}) = \mathcal{N}^{1/2} \exp[-S(E)/2]$$
 (3.11)

now appears as a zero mode of the operator H,

$$H\phi = 0, (3.12)$$

that has unit normalization,

$$(\phi, \phi) = 1.$$
 (3.13)

Except for this zero mode function, the remaining spectrum of H is positive. This is true because, for any function $\psi(\mathbf{p})$,

$$(\psi, H\psi) = \int \frac{d^{3}\mathbf{p}}{(2\pi\hbar)^{3}} \frac{\langle T\mathcal{A}(E)\rangle}{v} \times \left\{ \left[\hat{\mathbf{v}} \cdot \frac{\partial}{\partial \mathbf{p}} + \frac{v \mathcal{A}(E)}{2\langle T\mathcal{A}(E)\rangle} \right] \psi(\mathbf{p}) \right\}^{2} \geqslant 0, \quad (3.14)$$

since an examination of our results for the \mathcal{A} coefficients shows that $\langle T \mathcal{A}(E) \rangle \geqslant 0$. The equality in Eq. (3.14) holds only if

$$\left[\hat{\mathbf{v}} \cdot \frac{\partial}{\partial \mathbf{p}} + \frac{v \,\mathcal{A}(E)}{2\langle T \,\mathcal{A}(E) \rangle}\right] \psi(\mathbf{p}) = 0. \tag{3.15}$$

The spherically symmetric solution $\psi(\mathbf{p}) = \psi(|\mathbf{p}|)$ is clearly the previous zero mode function $\psi(\mathbf{p}) = \phi(E)$. Hence, within the class of isotropic solutions—the only class that is relevant to our work—there are no other zero modes of H and all its other eigenvalues are positive. Since the operator H is Hermitian,

$$\phi H = 0. \tag{3.16}$$

In view of this adjoint equation, it follows that

$$\phi \, e^{-H(t-t')} = \phi. \tag{3.17}$$

Except for this zero mode, we have shown that the other eigenvalues of the Hermitian operator H are positive. This positivity constraint must be obeyed, for otherwise the Fokker-Planck equation would have diverging "runaway" solutions at large times. The operator that projects out the zero mode is obviously the outer product of the zero mode vector with itself,

$$P = \phi \otimes \phi, \tag{3.18}$$

and we write the complement operator as

$$Q = 1 - P, (3.19)$$

where the first term in Eq. (3.19) is the unit operator on the function space. By definition, the operator P acts on an arbitrary function ψ as

$$P \psi(\mathbf{p}) = (\phi \otimes \phi)\psi(\mathbf{p}) = \phi(\mathbf{p})(\phi, \psi). \tag{3.20}$$

We now see that the unit operator in the form P + Q acting on g(E,t) in Eq. (3.9) produces

$$g(E,t) = \phi(\mathbf{p}) \int \frac{d^{3}p'}{(2\pi\hbar)^{3}} \phi(\mathbf{p}') \delta(E' - E_{0}) e^{S(E_{0})/2} \int_{-\infty}^{t} dt' s(t') + \int_{-\infty}^{t} dt' e^{-H(t-t')} Q \delta(E - E_{0}) e^{S(E_{0})/2} s(t').$$
(3.21)

The momentum integral in the first term of (3.21) is easy to evaluate.

$$\phi(\mathbf{p}) \int \frac{d^{3}\mathbf{p}'}{(2\pi\hbar)^{3}} \phi(\mathbf{p}') \delta(E' - E_{0}) e^{S(E_{0})/2}$$

$$= \mathcal{N} e^{-S(E)/2} \frac{\sqrt{2m^{3}E_{0}}}{2\pi^{2}\hbar^{3}}.$$
(3.22)

As for the second term, since the operator Q selects out the positive eigenvalues of H, an integration by parts can be performed to produce

$$\int_{-\infty}^{t} dt' \, e^{-H(t-t')} \, Q\delta \, (E - E_0) \, e^{S(E_0)/2} \, s(t')$$

$$= \frac{1}{H} \, Q\delta \, (E - E_0) \, e^{S(E_0)/2} \, s(t)$$

$$- \int_{-\infty}^{t} dt' \, e^{-H(t-t')} \, \frac{1}{H} \, Q\delta \, (E - E_0) \, e^{S(E_0)/2} \, \dot{s}(t').$$
(3.23)

We now assume that the source s(t) is adiabatically turned on and attains the constant value $s(t) = s_0$ at late times. In the asymptotic limit, the rate $\dot{s}(t)$ is, therefore, vanishingly small and the second term in Eq. (3.23) may be neglected. We may also replace s(t) by its asymptotic value s_0 in the first line. Hence, on multiplying g(E,t) by $\exp\{-S(E)/2\}$ to return to the function f(E,t), we obtain

$$f(E,t) = \mathcal{N} e^{-S(E)} \frac{\sqrt{2m^3 E_0}}{2\pi^2 \hbar^3} \int_{-\infty}^t dt' \, s(t') + \bar{f}(E), \quad (3.24)$$

where

$$\bar{f}(E) = e^{-S(E)/2} \frac{1}{H} Q\delta(E - E_0) e^{S(E_0)/2} s_0.$$
 (3.25)

Using Eq. (3.4), we can write this asymptotic late time solution more suggestively as

$$f(E,t) = n(t) f_{\infty}(E) + \bar{f}(E),$$
 (3.26)

with $f_{\infty}(E) = \mathcal{N} e^{-S(E)}$. We emphasize that expression (3.26) is the asymptotic late-time solution to the inhomogeneous Fokker-Planck equation since the term involving the derivative $\dot{s}(t)$ is omitted.

C. Energy deposition

Before presenting an explicit version of the formal solution (3.26), we pause to describe its physical interpretation and

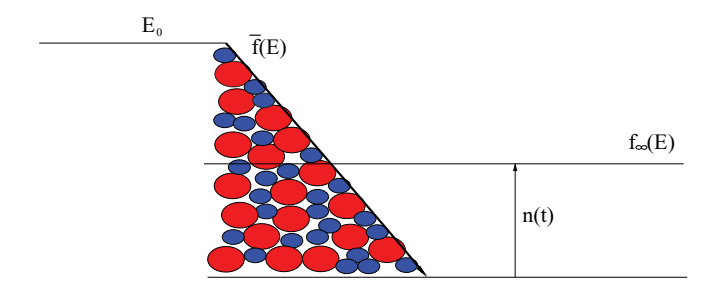


FIG. 2. (Color) The waterfall analogy: The small blue rocks represent the plasma electrons while the larger red rocks are the plasma ions. The motion of the "water" represents the evolution of the projectile ions that are injected into the background plasma. As "water" falls down the electron-ion slope at a constant rate determined by $\bar{f}(E)$, energy is deposited into electrons and ions—in the analogy, the rocks are heated. At the bottom of the fall is a lake into which the excess "water" drains and whose height n(t) rises linearly with time. In the analogy, the lake represents the final distribution $f_{\infty}(E)$.

its relation to the ways in which the slowing charged particle deposits its energy to the background plasma. At large times, the phase-space density has the time-independent contribution $f_{\infty}(E) = \mathcal{N} \exp[-S(E)]$ into which any set of initial projectile particles must relax, and the first term of (3.26) describes this distribution normalized to the correct density n(t). There remains a time-independent part $\bar{f}(E)$ that describes the stationary process of particles losing energy to the background electrons and ions as particles pass through "energy bins" from the initial energy E_0 to the final asymptotic distribution. The situation described here can be pictured as the flow of water over a rocky waterfall that slows the motion of the water as it descends. The initial rate of flow of the river corresponds to the rate $\dot{n}(t)$; the height h of the waterfall giving a potential energy proportional to gh corresponds to the initial energy E_0 . The energy dissipated in the fall corresponds to the energies lost to the ions and electrons (large and small rocks respectively). The final flow into a horizontal lake corresponds to the buildup of the particles in their final distribution described by $f_{\infty}(E)$. This analogy is depicted in Fig. 2.

D. Energy splitting

On inserting the form (3.26) into Eq. (3.3), we can identify the asymptotic constant rates of energy loss as

$$\bar{E}\,\dot{n}_{\infty} = (E_0 - E_1 - E_e)\,\dot{n}_{\infty},$$
 (3.27)

in which

$$\frac{E_{\mathrm{I},e}}{E_0} = \frac{1}{\dot{n}_{\infty} E_0} \int \frac{d^3 \mathbf{p}}{(2\pi\hbar)^3} v \,\mathcal{A}_{\mathrm{I},e}(E) \left(1 + T_{\mathrm{I},e} \,\frac{\partial}{\partial E}\right) \,\bar{f}(E). \tag{3.28}$$

Here, we write a single generic equation to represent, in fact, two separate equations: one for the ions and one for the electrons by the simple expedient of using the double subscript notation I, e. The constant fractions of the original energy E_0 deposited into ionic energy E_1 and electronic energy E_e are given in Eq. (3.28)—the energy losses analogous to those of the water passing through the rocky waterfall.

E. Plasma heating and energy exchange

Part of E_0 goes into energies lost to the ions and electrons, with the remainder being the average energy \bar{E} of an projectile particle in the final $f_{\infty}(E)$ ensemble. For a background plasma with the ions and electrons at a common temperature T, this final ensemble is just the Maxwell-Boltzmann distribution, $\bar{E} = 3T/2$, and the result (3.27) becomes obvious.

When the electrons and ions have the same temperature $T=T_e=T_1$, the slowing down of fast particles in the plasma gives a steady-state heating rate per unit volume $\mathcal{P}=(E_1+E_e)\dot{n}_{\infty}$. This heating raises the temperature T of the plasma, but, in most cases, the rate of this heating is small in comparison with the slowing down time of the fast projectile particles, and so our quasi-steady-state computation is valid, with the temperature treated as a slowing varying function in our formulas.

When the electrons and ions have different temperatures T_e and T_i , the situation may differ markedly. In addition to the overall plasma heating \mathcal{P} , the final ensemble of the projectile particles works to bring the electrons and ions to a common temperature. Returning to Eq. (3.3), we see that the final ensemble contribution produces energy density transfer rates to the ions and electrons given by

$$\dot{\mathcal{E}}_{I,e}(t) = + \int \frac{d^3 \mathbf{p}}{(2\pi\hbar)^3} v \,\mathcal{A}_{I,e}(E) \left(1 + T_{I,e} \,\frac{\partial}{\partial E} \right) \mathcal{N}$$

$$\exp[-S(E)] \, n(t). \tag{3.29}$$

Carrying out the energy derivatives yields

$$\dot{\mathcal{E}}_{\rm I}(t) = -(T_{\rm I} - T_{\rm e}) C_{\rm I,e}^{\alpha} \tag{3.30}$$

and

$$\dot{\mathcal{E}}_e(t) = -(T_e - T_1) C_{e_1}^{\alpha},$$
 (3.31)

with identical coefficients

$$C_{1e}^{\alpha} = C_{e1}^{\alpha} = n(t) \int \frac{d^{3}\mathbf{p}}{(2\pi\hbar)^{3}} v \frac{\mathcal{A}_{I}(E) \mathcal{A}_{e}(E)}{\langle T \mathcal{A} \rangle} \mathcal{N} \exp[-S(E)].$$
(3.32)

Hence,

$$\dot{\mathcal{E}}_{I}(t) + \dot{\mathcal{E}}_{e}(t) = 0, \qquad (3.33)$$

and there is no net heating of the plasma. This process only brings the ions and electrons to a common temperature.

When only a relatively small number of projectile particles have slowed into their final $f_{\infty}(E)$ distribution, they may be neglected, and the thermal relaxation rate coefficient is well approximated by⁷

$$C_{1e} = C_{e1} = \frac{\kappa_e^2}{2\pi} \,\omega_1^2 \sqrt{\frac{m_e}{2\pi \, T_e}} \, \frac{1}{2} \left[\ln\left(\frac{8T_e^2}{\hbar^2 \,\omega_e^2}\right) - \gamma - 1 \right]. \tag{3.34}$$

Here

$$\kappa_e^2 = \frac{e^2 \, n_e}{T_e} \tag{3.35}$$

⁷This is the sum of Eqs. (12.44) and (12.57) in BPS [3] as quoted in Eq. (12.12) except that a simple transcription error was made in the sum quoted in BPS in that the $-\gamma - 2$ in Eq. (12.12) should be replaced by $-\gamma - 1$.

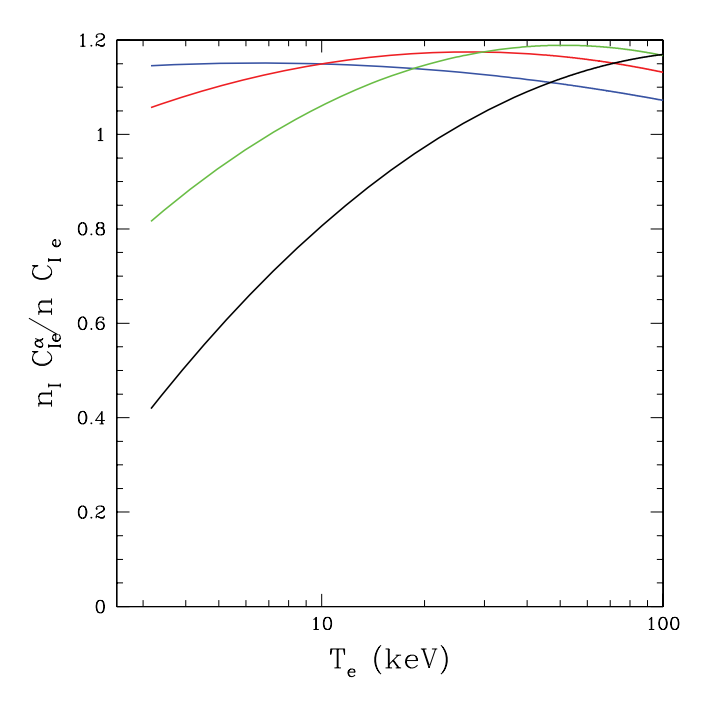


FIG. 3. (Color online) The ratio $n_1 C_{1e}^{\alpha}/n C_{1e}$ as a function of the electron temperature for an equimolar DT plasma with an electron density of 1.0×10^{24} cm⁻³ for ion temperatures of 3, 10, 30, and 100 keV. The curves for increasing ion temperatures T_1 have increasing values for small electron temperatures T_e , although they do cross at larger T_e .

is the squared electron Debye wave number, and

$$\omega_a^2 = \frac{e_a^2 n_a}{m_a} \tag{3.36}$$

is the definition of the squared plasma frequency for particle a, with the electron squared plasma frequency ω_e^2 specified by a=e, while the total squared ionic plasma frequency ω_1^2 is the sum over all the ions in the plasma

$$\omega_{\rm I}^2 = \sum_i \omega_i^2. \tag{3.37}$$

In numerical terms, for an equimolar DT plasma,

$$C_{1e} = 3.13 \times 10^{-26} n_e^2 T_e^{-3/2}$$

$$\times \left[\ln \left(5.80 \times 10^{27} \frac{T_e^2}{n_e} \right) - 1.58 \right] \text{cm}^{-3} \, \text{ps}^{-1}, \quad (3.38)$$

in which the electron density n_e is measured in cm⁻³, the electron temperature T_e in keV, and the overall units are $(1.0 \text{ cm}^{-3})/(1.0 \times 10^{-12} \text{ s})$ as indicated.

The total rate coefficient for electron-ion thermal relaxation is the sum $C_{1e} + C_{1e}^{\alpha}$. It is of interest to compare C_{1e}^{α} to C_{1e} . Since C_{1e}^{α} is proportional to the number density n(t) of projectile particles in their final distribution $f_{\infty}(E)$, this comparison can be made independent of this density by evaluating the ratio of $C_{1e}^{\alpha}/n(t)$ to C_{1e}/n_1 . In Fig. 3 we plot this dimensionless ratio as a function of the electron temperature T_e for various values of the ion temperature T_1 ranging from 3 to 100 keV at an electron density $n_e = 1.0 \times 10^{24}$ cm⁻³. Explicit calculation shows that the dependence of this ratio

upon the electron density n_e is weak. As n_e is increased from $1.0 \times 10^{24} \, \mathrm{cm}^{-3}$ to $1.0 \times 10^{26} \, \mathrm{cm}^{-3}$, the greatest change in the ratio occurs for $T_1 \gg T_e$: for $T_1 = 100 \, \mathrm{keV}$ and $T_e = 3 \, \mathrm{keV}$, the ratio increases by 20%.

We must add the caveat, already noted in the Introduction, that the preceding discussion applies only to the case in which the final α particle population is not large. Hence, although in some cases the ratios shown in Fig. 3 are of order one, the net effect of this new mechanism must be relatively small.

IV. EXPLICIT SOLUTION

A. General development

We turn now to the explicit construction of the function $\bar{f}(E)$ from the formal expression (3.25). We start by multiplying Eq. (3.25) by the (velocity \sim momentum) differential operator structure in Eq. (3.1). Passing this operator through the factor $\exp[-S(E)/2]$ is equivalent to the similarity transformation that converts it into the operator H. Hence,

$$-\frac{\partial}{\partial \mathbf{p}} \cdot \hat{\mathbf{v}} \left[\mathcal{A} + \langle T \mathcal{A}(E) \rangle \frac{\hat{\mathbf{v}}}{v} \cdot \frac{\partial}{\partial \mathbf{p}} \right] \bar{f}(E)$$

$$= e^{-S(E)/2} Q e^{+S(E)/2} \delta (E - E_0) s_0, \tag{4.1}$$

and remembering Eqs. (2.16), we see that this is equivalent to

$$-\frac{\partial}{\partial v} \frac{v^{2}}{m} \left[\mathcal{A} + \langle T \mathcal{A}(E) \rangle \frac{\partial}{\partial E} \right] \bar{f}(E)$$

$$= v^{2} e^{-S(E)/2} Q e^{+S(E)/2} \delta (E - E_{0}) s_{0}$$

$$= \delta (E - E_{0}) \frac{2E_{0}}{m} s_{0} - v^{2} \mathcal{N} e^{-S(E)} \frac{\sqrt{2m^{3} E_{0}}}{2\pi^{2} \hbar^{3}} s_{0}. \quad (4.2)$$

In the second equality we employed the definitions (3.18) and (3.19) of the operators P and Q and in the last line used the result (3.22). Obviously, a trivial first integral of this differential equation exists. Since the constant of integration must be chosen to make $\bar{f}(E)$ vanish at large E, this first integral reads

$$\begin{split} & \left[\mathcal{A}(E) + \langle T \mathcal{A}(E) \rangle \frac{\partial}{\partial E} \right] \bar{f}(E) \\ & = \frac{s_0}{E} \sqrt{\frac{mE_0}{2}} \left[\theta \left(E_0 - E \right) - \int_E^{\infty} dE' \, \frac{m \sqrt{2mE'}}{2\pi^2 \hbar^3} \, \mathcal{N}e^{-S(E')} \right], \end{split} \tag{4.3}$$

where $\theta(x)$ is the unit step function that vanishes for x < 0. Note that, in view of the normalization (2.20),

$$\int_{0}^{\infty} dE' \frac{m\sqrt{2mE'}}{2\pi^{2}\hbar^{3}} \mathcal{N}e^{-S(E')} = \int \frac{d^{3}\mathbf{p}'}{(2\pi\hbar)^{3}} \mathcal{N}e^{-S(E')} = 1,$$
(4.4)

and so the sum of the terms in the square brackets in Eq. (4.3) vanishes when $E \to 0$. This is in accord with the fact that these terms on the right of Eq. (4.3) were produced by the integral of a derivative on the left-hand side of Eq. (4.2), a derivative of a quantity that vanishes at both E = 0 and $E = \infty$. Moreover, since the square brackets vanishes at E = 0, the right-hand side of Eq. (4.3) is finite at this end point as it must be.

At this juncture, it is convenient to remember the definition (3.5) of \dot{n}_{∞} , which can be expressed as

$$\sqrt{\frac{mE_0}{2}} \, s_0 = \frac{\pi^2 \hbar^3}{mE_0} \, E_0 \, \dot{n}_\infty, \tag{4.5}$$

and to simplify the notation by writing

$$\overline{\mathcal{N}} = \frac{m\sqrt{2m}}{2\pi^2\hbar^3}\,\mathcal{N},\tag{4.6}$$

so we have

$$\int_0^\infty dE' \sqrt{E'} \, \overline{\mathcal{N}} \, e^{-S(E')} = 1. \tag{4.7}$$

Thus, Eq. (4.3) now reads,

$$\left[\mathcal{A}(E) + \langle T\mathcal{A}(E) \rangle \frac{\partial}{\partial E}\right] \frac{\bar{f}(E)}{E_0 \dot{n}_{\infty}}
= \frac{\pi^2 \hbar^3}{m E_0 E} \left[\theta \left(E_0 - E\right) - \int_E^{\infty} dE' \sqrt{E'} \, \overline{\mathcal{N}} \, e^{-S(E')}\right].$$
(4.8)

To solve this differential equation, we set

$$\bar{f}(E) = e^{-S(E)} \,\bar{g}(E),$$
 (4.9)

because then

$$\left[\mathcal{A}(E) + \langle T\mathcal{A}(E) \rangle \frac{\partial}{\partial E}\right] \bar{f}(E) = e^{-S(E)} \langle T\mathcal{A}(E) \rangle \frac{\partial}{\partial E} \bar{g}(E). \tag{4.10}$$

Since the integrating factor involves $\exp\{+S(E)\}$, which exponentially increases without bound as the energy increases, to obtain a finite well-defined result we must integrate over the range E' = 0 to E' = E and obtain

$$\begin{split} \frac{\bar{g}(E)}{E_0 \, \dot{n}_{\infty}} &= \frac{\pi^2 \hbar^3}{m E_0} \, \int_0^E \frac{dE'}{E'} \, \frac{e^{+S(E')}}{\langle T \mathcal{A}(E') \rangle} \\ &\times \left[\theta(E_0 - E') \, - \int_{E'}^\infty dE'' \sqrt{E''} \, \overline{\mathcal{N}} \, e^{-S(E'')} \right]. \end{split} \tag{4.11}$$

B. Equal electron and ion temperatures

The case in which the ions and electrons have the same temperature, $T_1 = T_e = T = \beta^{-1}$, is simple in several respects. First, it is physically simpler because the final distribution of the stopping charged particles is the Maxwell-Boltzmann thermal equilibrium distribution of the background plasma,

$$\exp[-S(E)] = \exp\left(-\frac{E}{T}\right). \tag{4.12}$$

Thus, the energy transfer processes (3.29) do not appear because, with Eq. (4.12) holding, the combination in the large parentheses of Eq. (3.29) annihilates $\exp[-S(E)]$. Thus, only the energy partitions E_1 and E_e need to be examined, and these obey the obvious sum rule

$$\frac{3}{2}T = E_0 - E_1 - E_e, \tag{4.13}$$

to which Eq. (3.27) reduces. Second, it is mathematically simpler because there is no need to find an explicit solution to Eq. (4.11) because Eq. (4.8) reduces to

$$\left(1 + T \frac{\partial}{\partial E}\right) \frac{\bar{f}(E)}{E_0 \dot{n}_{\infty}}$$

$$= \theta \left(E_0 - E\right) \frac{1}{E \mathcal{A}(E)} \frac{\pi^2 \hbar^3}{m E_0}$$

$$- \frac{1}{E_0 E \mathcal{A}(E)} \left(\frac{2\pi \hbar^2}{m T}\right)^{3/2} \int_E^{\infty} dE' \sqrt{2m E'} e^{-\beta E'}.$$
(4.14)

The operation in the square brackets that acts on $\bar{f}(E)$ on the left-hand side of this equation is just that which appears in the energy partitions (3.28).

Placing this expression into the energy partitions Eq. (3.28) and changing the momentum integration into an integration over energy expresses the fractional energy loss into ions and electrons as

$$\frac{E_{1,e}}{E_0} = \int_0^{E_0} \frac{dE}{E_0} \frac{\mathcal{A}_{1,e}(E)}{\mathcal{A}(E)} - \int_0^{\infty} \frac{dE}{E_0} \frac{\mathcal{A}_{1,e}(E)}{\mathcal{A}(E)} \frac{2\beta^{3/2}}{\sqrt{\pi}} \int_E^{\infty} dE' \sqrt{E'} e^{-\beta E'}.$$
(4.15)

Adding the separate results for the ions and electrons gives

$$E_{1} + E_{e} = E_{0} - \frac{2 \beta^{3/2}}{\sqrt{\pi}} \int_{0}^{\infty} dE \int_{E}^{\infty} dE' \sqrt{E'} e^{-\beta E'}$$

$$= E_{0} - \frac{3}{2} T. \tag{4.16}$$

This is just the obvious result of energy conservation previously stated in Eq. (3.27).

The results (4.15) can be simplified for their explicit evaluation. Writing these results with a trivial rearrangement of the terms presents them as

$$\frac{E_{i,e}}{E_0} = \int_0^{E_0} \frac{dE}{E_0} \frac{\mathcal{A}_{i,e}(E)}{\mathcal{A}(E)} \left(1 - \frac{2\beta^{3/2}}{\sqrt{\pi}} \int_E^{\infty} dE' \sqrt{E'} e^{-\beta E'} \right) \\
- \int_{E_0}^{\infty} \frac{dE}{E_0} \frac{\mathcal{A}_{i,e}(E)}{\mathcal{A}(E)} \frac{2\beta^{3/2}}{\sqrt{\pi}} \int_E^{\infty} dE' \sqrt{E'} e^{-\beta E'}.$$
(4.17)

As we shall see, the second line in Eq. (4.17) is exponentially small. Hence, it suffices to use the simple bounds

$$\frac{\mathcal{A}_{i}(E)}{\mathcal{A}(E)} = \frac{\mathcal{A}_{i}(E)}{\mathcal{A}_{i}(E) + \mathcal{A}_{e}(E)} \leqslant 1, \tag{4.18}$$

and, similarly,

$$\frac{\mathcal{A}_e(E)}{\mathcal{A}(E)} \leqslant 1. \tag{4.19}$$

Using these bounds, we encounter

$$-\int_{E_0}^{\infty} \frac{dE}{E_0} \frac{2 \beta^{3/2}}{\sqrt{\pi}} \int_{E}^{\infty} dE' \sqrt{E'} e^{-\beta E'}$$

$$= -\frac{2 \beta^{3/2}}{\sqrt{\pi}} \int_{E_0}^{\infty} dE' \sqrt{E'} e^{-\beta E'} \int_{E_0}^{E'} \frac{dE}{E_0}$$

$$= -\frac{2 \beta^{3/2}}{\sqrt{\pi}} \int_{E_0}^{\infty} dE' \sqrt{E'} e^{-\beta E'} \left(\frac{E'}{E_0} - 1\right). \quad (4.20)$$

The variable change $E' = E_0(x + 1)$ presents this as

$$-\frac{2\beta^{3/2}}{\sqrt{\pi}} E_0^{3/2} e^{-\beta E_0} \int_0^\infty dx \, (1+x)^{1/2} x \, e^{-\beta E_0 x}$$

$$\simeq -\frac{2}{\sqrt{\pi}} \frac{1}{\sqrt{\beta E_0}} e^{-\beta E_0}, \tag{4.21}$$

with the evaluation on the right-hand side following from the fact that $\beta E_0 \gg 1$ so only small x regions contribute, justifying the replacement $(1+x)^{1/2} \to 1$. Hence, we indeed find that the second line in Eq. (4.17) is exponentially small.

Since

$$\frac{2\beta^{3/2}}{\sqrt{\pi}} \int_0^\infty dE' \sqrt{E'} e^{-\beta E'} = 1, \tag{4.22}$$

we may now write the result (4.17) as

$$\frac{E_{\rm I, e}}{E_0} = \int_0^{E_0} \frac{dE}{E_0} \frac{\mathcal{A}_{\rm I, e}(E)}{\mathcal{A}(E)} \, \psi(\beta \, E),\tag{4.23}$$

in which

$$\psi(x) = \frac{2}{\sqrt{\pi}} \int_0^x dt \, t^{1/2} \, e^{-t}. \tag{4.24}$$

Writing $\exp\{-t\} = -d \exp\{-t\}/dt$ and integrating by parts yields

$$\psi(x) = \frac{2}{\sqrt{\pi}} \int_0^x dt \, \frac{1}{2} \, t^{-1/2} \, e^{-t} - \sqrt{\frac{4 \, x}{\pi}} \, e^{-x}. \quad (4.25)$$

The variable change $t = y^2$ identifies the integral here as the error function,

$$\operatorname{erf}(\sqrt{x}) = \frac{2}{\sqrt{\pi}} \int_0^{\sqrt{x}} dy \, e^{-y^2}, \tag{4.26}$$

and so

$$\psi(x) = \text{erf}(\sqrt{x}) - \sqrt{\frac{4x}{\pi}} e^{-x}.$$
 (4.27)

These are the results quoted in the preceding paper [2].

C. Differing electron and ion temperatures

As we have seen, when the ion and electron temperatures of the background plasma differ, $T_1 \neq T_e$, both the physical interpretation is richer and the mathematics becomes more difficult. With different temperatures, there is the additional

physical process in which the final distribution of projectile particles works to bring the electrons and ions into thermal equilibrium at a common temperature $T = T_1 = T_e$. Moreover, mathematically, we must now work with Eq. (4.11).

We use Eq. (4.11) to return to the $\bar{f}(E)$ function and insert the result for $\bar{f}(E)$ into Eq. (3.28) to compute E_1/E_0 and E_e/E_0 . To simplify the resulting formulas, and place them in a form that parallels those for the previous equal ion-electron temperature case, we note that

$$\begin{cases}
\mathcal{A}_{I}(E) \\
\mathcal{A}_{e}(E)
\end{cases} \left[1 + \left\{ \frac{T_{I}}{T_{e}} \right\} \frac{d}{dE} \right] e^{-S(E)} \\
= \left\{ \frac{+}{-} \right\} (T_{e} - T_{I}) \frac{\mathcal{A}_{I}(E) \mathcal{A}_{e}(E)}{\langle T \mathcal{A}(E) \rangle} e^{-S(E)}. \quad (4.28)
\end{cases}$$

Hence, with the definition

$$G(T_{I}, T_{e}; E_{0})$$

$$= \int_{0}^{\infty} dE E \frac{\mathcal{A}_{I}(E)\mathcal{A}_{e}(E)}{\langle T\mathcal{A}(E) \rangle} e^{-S(E)} \int_{0}^{E} \frac{dE'}{E'} \frac{e^{+S(E')}}{\langle T\mathcal{A}(E') \rangle}$$

$$\times \left[\theta(E_{0} - E') - \int_{E'}^{\infty} dE'' \sqrt{E''} \overline{\mathcal{N}} e^{-S(E'')} \right], \quad (4.29)$$

the energy loss fractions may be expressed as

$$\frac{E_{\rm I}}{E_0} = \left(\frac{T_e - T_{\rm I}}{E_0}\right) G(T_{\rm I}, T_e; E_0) + \int_0^\infty \frac{dE}{E_0} \frac{T_{\rm I} \mathcal{A}_{\rm I}(E)}{\langle T \mathcal{A}(E') \rangle} \times \left[\theta \left(E_0 - E\right) - \int_E^\infty dE' \sqrt{E'} \, \overline{\mathcal{N}} \, e^{-S(E')}\right] \tag{4.30}$$

and

$$\frac{E_e}{E_0} = \left(\frac{T_1 - T_e}{E_0}\right) G(T_1, T_e; E_0) + \int_0^\infty \frac{dE}{E_0} \frac{T_e \mathcal{A}_e(E)}{\langle T \mathcal{A}(E') \rangle} \times \left[\theta \left(E_0 - E\right) - \int_E^\infty dE' \sqrt{E'} \, \overline{\mathcal{N}} \, e^{-S(E')}\right]. (4.31)$$

The second lines in the results (4.30) and (4.31) are straightforward generalizations of the common ion and electron temperature form (4.15). The first lines of the new results (4.30) and (4.31) cancel when they are summed, so

$$E_{\rm I} + E_e = + \int_0^{E_0} dE - \overline{\mathcal{N}} \int_0^\infty dE \int_E^\infty dE' \sqrt{E'} e^{-S(E')}.$$
(4.32)

On interchanging the order of integration,

$$\int_{0}^{\infty} dE \int_{E}^{\infty} dE' \sqrt{E'} e^{-S(E')}$$

$$= \int_{0}^{\infty} dE' \sqrt{E'} e^{-S(E')} \int_{0}^{E'} dE$$

$$= \int_{0}^{\infty} dE' E' \sqrt{E'} e^{-S(E')}.$$
(4.33)

Hence, on passing from an integration over energy to an equivalent momentum integral and reverting to the corresponding

normalization factor \mathcal{N} , we have

$$E_{\rm I} + E_e = E_0 - \int \frac{d^3 \mathbf{p}}{(2\pi\hbar)^3} E \mathcal{N} e^{-S(E)}$$
 (4.34)

or, in view of Eq. (2.26),

$$E_{\rm I} + E_{\rm e} = E_0 - \bar{E},\tag{4.35}$$

in which \bar{E} is the average energy to which a projectile particle relaxes. This result is in accord with the previous Eq. (3.27).

The final energy integrals in Eqs. (4.30) and (4.31) run from E=0 to $E\to\infty$. In each case, the final integration region involves the exponentially small factor $\exp[-S(E_0)] \simeq \exp(-E_0/\bar{T})$, where \bar{T} is a typical plasma temperature. This is a very small factor, and hence this upper portion of the integration region may be safely neglected to write the results as

$$\frac{E_{1}}{E_{0}} = \left(\frac{T_{e} - T_{1}}{E_{0}}\right) G(T_{1}, T_{e}; E_{0})$$

$$+ \int_{0}^{E_{0}} \frac{dE}{E_{0}} \frac{T_{1} \mathcal{A}_{1}(E)}{\langle T \mathcal{A}(E') \rangle} \left[1 - \int_{E}^{\infty} dE' \sqrt{E'} \overline{\mathcal{N}} e^{-S(E')}\right]$$

$$= \left(\frac{T_{e} - T_{1}}{E_{0}}\right) G(T_{1}, T_{e}; E_{0})$$

$$+ \int_{0}^{E_{0}} \frac{dE}{E_{0}} \frac{T_{1} \mathcal{A}_{1}(E)}{\langle T \mathcal{A}(E') \rangle} \int_{0}^{E} dE' \sqrt{E'} \overline{\mathcal{N}} e^{-S(E')} \quad (4.36)$$

and

$$\frac{E_e}{E_0} = \left(\frac{T_1 - T_e}{E_0}\right) G(T_1, T_e; E_0)
+ \int_0^{E_0} \frac{dE}{E_0} \frac{T_e \mathcal{A}_e(E)}{\langle T \mathcal{A}(E') \rangle} \int_0^E dE' \sqrt{E'} \overline{\mathcal{N}} e^{-S(E')}.$$
(4.37)

Here we have invoked the sum rule (4.7) to write the second equalities above.

The work in Appendix C shows that the function G can be approximated, with an accuracy of a few percentages, by

$$G(T_{1}, T_{e}; E_{0})$$

$$= \int_{0}^{E_{0}} dE E \frac{\mathcal{A}_{1}(E)\mathcal{A}_{e}(E)}{\langle T\mathcal{A}(E)\rangle} e^{-S(E)} \int_{0}^{E} \frac{dE'}{E'} \frac{e^{+S(E')}}{\langle T\mathcal{A}(E')\rangle}$$

$$\times \int_{0}^{E'} dE'' \sqrt{E''} \overline{\mathcal{N}} e^{-S(E'')} + \frac{\mathcal{A}_{1}(E_{0})\mathcal{A}_{e}(E_{0})}{\mathcal{A}^{2}(E_{0})}. \quad (4.38)$$

Since the integration in the first line is over the finite interval $(0, E_0)$ and since it involves only nested integrals, rather than a three-dimensional integral with an arbitrary integrand that involves an general function of three variables, its numerical evaluation is not difficult.

V. SUMMARY AND CONCLUSION

We have developed a formalism that enables the calculations of the energy fractions that a fast particle deposits to the ions and electrons when it slows down in a plasma of ions and electrons that have different temperatures. Such calculations have not been done previously. Our work applies to background plasmas that are weakly to moderately coupled—the range of validity of this restriction was discussed in the

Introduction. Using the explicit forms for the A coefficients reviewed in Appendix A, Eqs. (4.36) and (4.38) enable the explicit computation of the energy ratios E_1/E_0 that are presented in the preceding paper [2].

If the ions are not in thermal equilibrium with the electrons, a fast particle ends in a "schizophrenic" distribution $f_{\infty}(E)$ which we explicitly compute in Sec. III B. As described in Sec. III E, this final nonthermal distribution of the projectile particles provides a mechanism to bring the differing electron and ion temperatures to a final common temperature, a process that now appears in addition to the usual electron-ion relaxation interaction.

APPENDIX A: THE A COEFFICIENTS

The Fokker-Planck equation described in the text involves two scalar coefficient functions with only one of them, the \mathcal{A} coefficient, entering into our problem of the partition of the energy loss of a fast charged particle into the ions and electrons in the plasma. The Fokker-Planck equation, and the coefficients $\mathcal{A}_{\scriptscriptstyle \rm I}$ and $\mathcal{A}_{\it e}$ coming from the ions and electrons that are needed for our problem, were discussed extensively in BPS [3]. There a method (see footnote [3]) was employed to compute the A_b which enables the short-distance. point Coulomb scattering to be joined with the long-distance, collective force in an unambiguous fashion that has no double counting. This method was used to evaluate the A_b both to leading and to subleading order—roughly speaking—to order $n \ln n$ and order n, where n is the plasma number density (made dimensionless by the adduction of suitable parameters). For completeness, we present here the results of BPS.

The coefficient for the interaction of a projectile particle of energy E or velocity v_p , $(E = m_p v_p^2/2)$ with the species b of the background plasma may conveniently be written as

$$\mathcal{A}_b(v_p) = \mathcal{A}_b^{c}(v_p) + \mathcal{A}_b^{\Delta Q}(v_p), \tag{A1}$$

which is the same as Eq. (10.25) of BPS, with

$$\mathcal{A}_b^{\mathsf{c}}(v_p) = \mathcal{A}_{b,\mathsf{s}}^{\mathsf{c}}(v_p) + \mathcal{A}_{b,\mathsf{R}}^{\mathsf{c}}(v_p), \tag{A2}$$

which is the same as Eq. (9.6) of BPS. Here $\mathcal{A}_b^c(v_p)$ has two terms. The first accounts for the hard Coulomb scattering in the classical limit, while the second accounts for the collective, long-distance effects, which are entirely classical. The term $\mathcal{A}_b^{\Delta Q}(v_p)$ is the quantum-mechanical correction to the scattering that vanishes in the limit in which Planck's constant vanishes, $\hbar \to 0$.

The first classical piece is given by

$$\mathcal{A}_{b,s}^{c}(v_{p}) = \frac{e_{p}^{2} \kappa_{b}^{2}}{4\pi} \left(\frac{\beta_{b} m_{b}}{2\pi}\right)^{1/2} v_{p} \int_{0}^{1} du \, u^{1/2} \exp\left(-\frac{1}{2} \beta_{b} m_{b} v_{p}^{2} u\right) \times \left[-\ln\left(\beta_{b} \frac{e_{p} e_{b}}{4\pi} K \frac{m_{b}}{m_{pb}} \frac{u}{1-u}\right) - 2\gamma + 2\right], \quad (A3)$$

which is contained in Eq. (9.5) of BPS.⁸ The reduced mass m_{pb} of the projectile (p) and plasma particle (b) is defined by

$$\frac{1}{m_{pb}} = \frac{1}{m_p} + \frac{1}{m_b}. (A4)$$

The long distance collective part of the classical contribution is given by

$$\mathcal{A}_{b,R}^{<}(v_p) = \frac{e_p^2}{4\pi} \frac{i}{2\pi} \int_{-1}^{1} d\cos\theta \cos\theta \frac{\rho_b(v_p\cos\theta)}{\rho_{\text{total}}(v_p\cos\theta)} \times F(v_p\cos\theta) \ln\left[\frac{F(v_p\cos\theta)}{K^2}\right], \quad (A5)$$

which is contained in Eq. (7.26) of BPS. Here $\rho_{\text{total}}(v)$ is the spectral weight,

$$\rho_{\text{total}}(v) = \sum_{b} \rho_{b}(v), \qquad (A6)$$

with

$$\rho_b(v) = \kappa_b^2 \sqrt{\frac{\beta_b m_b}{2\pi}} v \exp\left(-\frac{1}{2} \beta_b m_b v^2\right), \quad (A7)$$

as introduced in BPS Eqs. (7.9) and (7.10). With these definitions, the sum $\mathcal{A}_{b,s}^c + \mathcal{A}_{b,R}^c$ is independent of the arbitrary wave number K. The function $F(v_p \cos \theta)$ is related to the classical dielectric function $\epsilon(k,kv_p\cos\theta)$ by

$$k^{2} \epsilon(k, k v_{n} \cos \theta) = k^{2} + F(v_{n} \cos \theta). \tag{A8}$$

Here, consistent with our leading orders evaluation, the dielectric function corresponds to the classical limit of the

⁸In our notation, and in view of Eq. (2.7), the formulas given on page 32 of the *NRL Plasma Formulary* [6] for the rate of energy loss of particle p to ions b in the plasma corresponds to writing the complete $A_b(v_p)$ coefficient as

$$\mathcal{A}_{b}(v_{p}) = \frac{e_{p}^{2} \kappa_{b}^{2}}{4\pi} \left(\frac{\beta_{b} m_{b}}{2\pi}\right)^{1/2} v_{p} \ln \Lambda \int_{0}^{1} du \, u^{1/2} \exp\left(-\frac{1}{2} \beta_{b} m_{b} v_{p}^{2} u\right),$$

where $\ln \Lambda$ is a Coulomb logarithm. This formula is the same as Eq. (A3) except that the terms in the square brackets on the last line in Eq. (A3) are replaced by $\ln \Lambda$. The *NRL Plasma Formulary* expression does not contain the "terms under the logarithm," the terms of order n that BPS computed exactly. These are terms that are discussed in what follows.

⁹The wave number K, introduced by our method of dimensional continuation, corresponds roughly to the upper limit of the long-distance contributions and the lower limit of the short-distance contributions. Since K can be chosen arbitrarily, the result must be independent of its value. This is easy to prove: In view of Eq. (A10), the K dependence of Eq. (A5) appears in a integrand with $F(v_p \cos \theta) \ln K^{-2}$ multiplying remaining factors that are odd in $\cos \theta$. Hence, in view of Eq. (A11), one finds that the K dependence of Eq. (A5) is given by

$$\frac{e_p^2}{4\pi} \int_0^1 d\cos\theta \, \cos\theta \, \rho_b(v_p\cos\theta) \ln K^2.$$

The variable change $\cos \theta = u^{1/2}$ along with the definition (A7) of ρ_b now easily shows that this term precisely cancels the K dependence of Eq. (A3).

quantum ring sum. Hence, the complex-valued function F(v) is defined by

$$F(v) = -\int_{-\infty}^{\infty} du \, \frac{\rho_{\text{total}}(u)}{v - u + i\eta},\tag{A9}$$

with $\eta \to 0^+$. Note that, since $(x - i\eta)^{-1} - (x + i\eta)^{-1} = 2\pi i \, \delta(x)$, and since

$$\rho_b(-u) = -\rho_b(u),\tag{A10}$$

we have

$$F(v) - F(-v) = 2\pi i \ \rho_{\text{total}}(v). \tag{A11}$$

Equations (A8) and (A9) are the formulas (7.7) and (7.8) of BPS

The quantum correction is contained in Eq. (10.27) of BPS, and it reads

$$\mathcal{A}_{b}^{\Delta Q}(v_{p}) = -\frac{e_{p}^{2} \kappa_{b}^{2}}{4\pi} \left(\frac{\beta_{b} m_{b}}{2\pi}\right)^{1/2} \frac{1}{2} \int_{0}^{\infty} dv_{pb}$$

$$\times \left[2 \operatorname{Re} \psi(1 + i\eta_{pb}) - \ln \eta_{pb}^{2}\right]$$

$$\times \frac{1}{\beta_{b} m_{b} v_{p} v_{pb}} \left\{ \exp \left[-\frac{1}{2} \beta_{b} m_{b} (v_{p} - v_{pb})^{2}\right] \right.$$

$$\times \left(1 - \frac{1}{\beta_{b} m_{b} v_{p} v_{pb}}\right) + \exp \left[-\frac{1}{2} \beta_{b} m_{b} (v_{p} + v_{pb})^{2}\right]$$

$$\times \left(1 + \frac{1}{\beta_{b} m_{b} v_{p} v_{pb}}\right) \right\}. \tag{A12}$$

Here $\psi(z) = d \ln \Gamma(z)/dz$ and

$$\eta_{pb} = \frac{e_p e_b}{4\pi\hbar v_{pb}} \tag{A13}$$

is the dimensionless quantum coupling parameter. Note that we use the rationalized Gaussian units that were used by BPS in which the Coulomb potential energy between charges e_a and e_b a distance r_{ab} apart is given by $V = e_a e_b/(4\pi r_{ab})$.

The following figures illustrate the behavior of the \mathcal{A} coefficients for an equimolar DT plasma with an α -particle projectile of kinetic energy E. Figures 4 and 5 plot the electron and ion components \mathcal{A}_e , $\mathcal{A}_{\rm l}$ and their sum $\mathcal{A}=\mathcal{A}_e+\mathcal{A}_{\rm l}$ for a plasma with electron number density $n_e=1.0\times 10^{25}~{\rm cm}^{-3}$, electron temperature $T_e=10~{\rm keV}$, and ion temperatures of $T_{\rm l}=10~{\rm keV}$ and 100 keV. Figures 6 and 7 illustrate the number density scaling of the \mathcal{A} coefficients by plotting $\mathcal{A}_e(E)/n_e$ and $\mathcal{A}_{\rm l}(E)/n_e$, as a function of the α -particle energy E, over a wide range of electron densities: $n_e=10^{25}$, 10^{26} , and $10^{27}~{\rm cm}^{-3}$. As before, the electron temperature is $T_e=10~{\rm keV}$ and the ion temperatures are $T_{\rm l}=10~{\rm keV}$ and $T_{\rm l}=100~{\rm keV}$.

Because the \mathcal{A} coefficients are proportional to the Debye wave number squared, a quantity proportional to n_e , it is no surprise that \mathcal{A}_1 and \mathcal{A}_e approximately scale with n_e . The Debye wave number also appears inside the logarithm and the dielectric function, and for electrons this produces a much more pronounced effect than for the much heavier ions: While

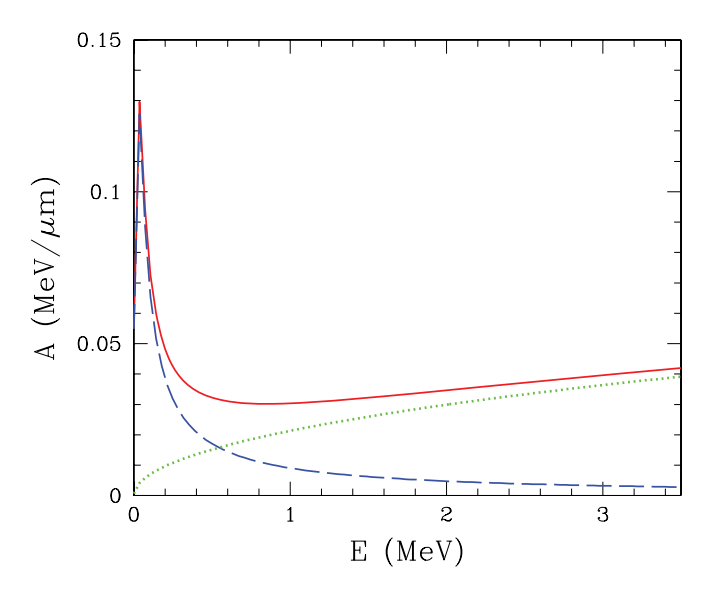


FIG. 4. (Color online) The coefficients $\mathcal{A}_{\rm I}(E)$ (dashed), $\mathcal{A}_{\rm e}(E)$ (dotted), and $\mathcal{A}(E)$ (solid) as functions of the kinetic energy E of an α particle projectile. The background plasma is equimolar DT with electron density $n_e=1.0\times 10^{25}~{\rm cm}^{-3}$ and electron-ion temperatures $T_e=10~{\rm keV}$ and $T_{\rm I}=10~{\rm keV}$.

 A_i/n_e is almost independent of n_e , the electron component A_e/n_e varies by a factor of 2 over the range of n_e .

APPENDIX B: ASYMPTOTIC LIMITS

We shall extract the large and small energy limits of the $\mathcal{A}_b(v_p)$ function for the various plasma species b from the general expressions in BPS [3]. The energy is given by $E=m_pv_p^2/2$, where m_p and v_p are the mass and speed of the particle moving through the plasma, the projectile p. We shall obtain the large and small limits of the projectile energy E as compared to a typical plasma temperature T.

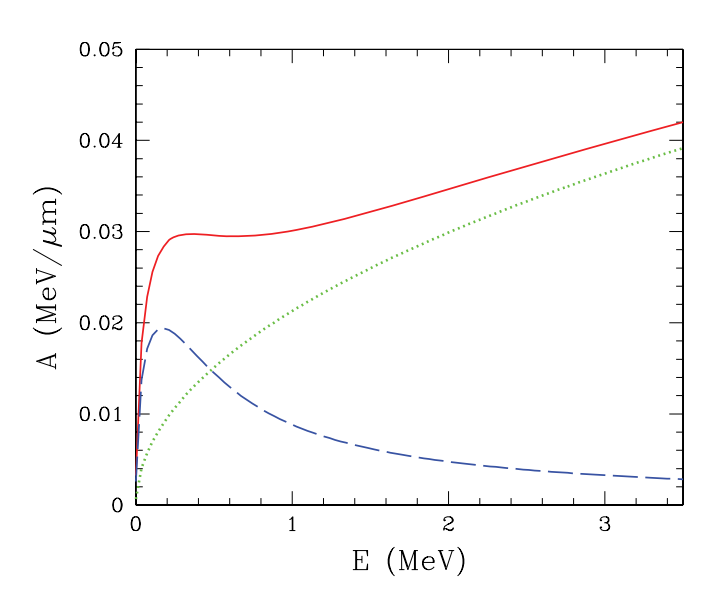


FIG. 5. (Color online) As in Fig. 4, except $T_e = 10$ keV and $T_1 = 100$ keV. The crossover energy $E = E_C$ where $A_e(E) = A_1(E)$ is about the same in both figures; however, the peak value of the coefficient A_1 is inversely proportional to T_1 .

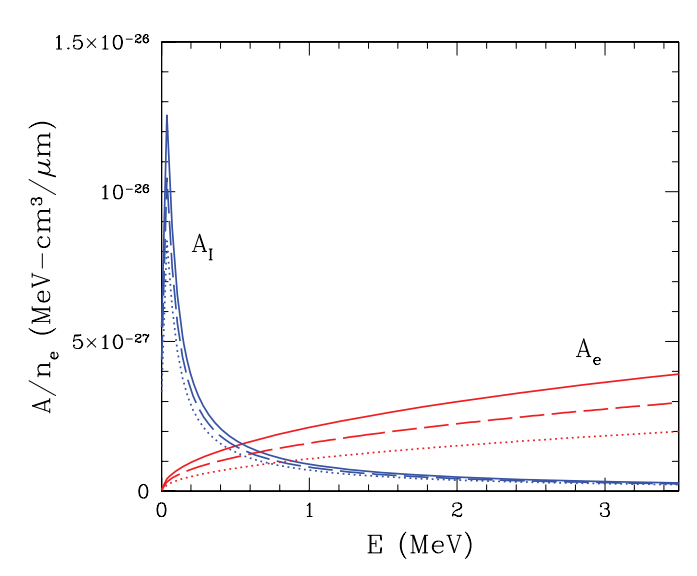


FIG. 6. (Color online) The \mathcal{A} coefficients for electrons and ions as a function of the α particle projectile energy E in an equimolar DT plasma with equal electron and ion temperatures, $T_e = T_1 = 10$ keV. The solid lines correspond to $n_e = 1.0 \times 10^{25}$ cm⁻³, the dashed lines to $n_e = 1.0 \times 10^{26}$ cm⁻³, and the dotted lines to $n_e = 1.0 \times 10^{27}$ cm⁻³. In each case, the A coefficient has been rescaled by the corresponding number density n_e . The slowly rising curves are those for \mathcal{A}_e , while the sharply peaked curves are for \mathcal{A}_1 .

1. $E \ll T$: Electrons and ions

In the low velocity limit, $A_b(v_p)$ vanishes linearly with v_p , and so we write

$$v_p \to 0: \mathcal{A}_b(v_p) = \frac{e_p^2 \kappa_b^2}{4\pi} \left(\frac{\beta_b m_b}{2\pi}\right)^{1/2} v_p \left(A_b^c + A_b^{\Delta Q}\right),\tag{B1}$$

with two constants A_b^c and $A_b^{\Delta Q}$. These two constants arise from the low velocity limit of the classical and quantum pieces of Eq. (A1). The classical piece has already been calculated

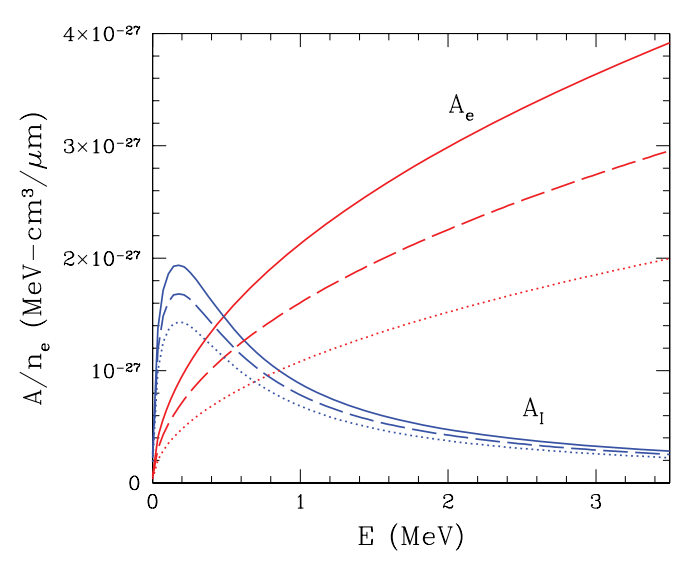


FIG. 7. (Color online) As in Fig. 6, except with $T_e = 10$ keV and $T_1 = 100$ keV.

by BPS, where it is contained in their Eq. (9.9), so there is no need to do it here. The result is

$$A_b^{\rm c} = \frac{2}{3} \left[\ln \left(\frac{16\pi}{e_p e_b \, \beta_b \kappa_{\rm D}} \frac{m_{pb}}{m_b} \right) - \frac{1}{2} - 2\gamma \right],$$
 (B2)

in which m_{pb} is the reduced mass defined in Eq. (A4) in the previous Appendix, and $\gamma = 0.577...$ is Euler's constant, and

$$\kappa_{\rm D}^2 = \sum_b \kappa_b^2 = \sum_b \beta_b \, e_b^2 \, n_b.$$
(B3)

To bring out the size of this classical part, we define a plasma coupling by

$$g_{pb} = \frac{e_p e_b \beta_b \kappa_D}{4\pi} = \frac{e_p e_b}{4\pi \lambda_D} \frac{1}{T_b},$$
 (B4)

in which $\lambda_D = 1/\kappa_D$ is the Debye length and $T_b = 1/\beta_b$ is the temperature of plasma species b. We may then write

$$A_b^c = \frac{2}{3} \left[\ln \left(\frac{4}{g_{pb}} \frac{m_{pb}}{m_b} \right) - \frac{1}{2} - 2\gamma \right],$$
 (B5)

which shows that $A_b^c > 0$, since g_{pb} must be small for our perturbative computation to hold. Note that when the electron and ion temperatures do not vastly differ, the ions dominate in the low velocity limit (B1) by a factor $(m_i/m_e)^{1/2}$. Moreover, since $\kappa^2 \sim 1/T$, this ionic contribution to the \mathcal{A} coefficient has the temperature factor $T_1^{-3/2}$ and, thus, increases as the ion temperature is lowered. The corrections to the low energy limit (B1) are of relative order E/T.

The low velocity limit of the quantum correction Eq. (A12) above was not previously calculated in BPS because there the low velocity limit of dE/dx was used only to compare with a computer simulation involving classical dynamics, and, therefore, the quantum correction was not needed. The needed quantum part is contained in Eq. (10.27) of BPS which provides the limit

$$v_p \to 0 : A_b^{\Delta Q} = -\frac{1}{3} \beta_b m_b \int_0^\infty dv_{pb} \, v_{pb} \exp\left(-\frac{1}{2} \beta_b m_b v_{pb}^2\right) \times \left[2 \operatorname{Re} \psi (1 + i \eta_{pb}) - \ln \eta_{pb}^2\right].$$
 (B6)

To bring out the character of Eq. (B6), we introduce a thermal velocity \bar{v}_b by

$$\frac{1}{2}\beta_b \, m_b \bar{v}_b^2 = \frac{3}{2} \tag{B7}$$

and a corresponding quantum parameter

$$\bar{\eta}_{pb} = \frac{e_p e_b}{4\pi \hbar \bar{v}_b}.$$
 (B8)

We then change the integration variable,

$$v_{pb} = \frac{e_p e_b}{4\pi\hbar \, \eta_{pb}} = \frac{e_p e_b}{4\pi\hbar} \, u = \bar{\eta}_{pb} \, \bar{v}_b \, u,$$
 (B9)

to obtain

$$\begin{split} A_b^{\Delta Q} &= A_b^{\Delta Q}(\bar{\eta}_{pb}) = -\bar{\eta}_{pb}^2 \, \int_0^\infty du \, u \, \exp\left(-\frac{3}{2}\bar{\eta}_{pb}^2 \, u^2\right) \\ &\times \left[2 \operatorname{Re} \psi \left(1 + \frac{i}{u}\right) + \ln u^2\right]. \end{split} \tag{B10}$$

If we introduce the Bohr radius $a_0 = 4\pi\hbar^2/e^2m_e$ and use the average squared thermal velocity definition (B7), we can write

$$\bar{\eta}_{pb}^2 = \frac{1}{3} \left(\frac{e_p e_b}{e^2} \right)^2 \frac{m_b}{m_e} \frac{1}{T_b} \frac{e^2}{4\pi a_0} \simeq \frac{1}{3} \left(\frac{e_p e_b}{e^2} \right)^2 \frac{m_b}{m_e} \frac{27 \text{eV}}{T_b}.$$
(B11)

Thus, for the charge and mass of a typical projectile particle such as an α particle and for a typical hot plasma, we see that for the electrons in the plasma $\bar{\eta}_{pe}^2 \ll 1$, while for the ions in the plasma $\bar{\eta}_{pi}^2 \gg 1$ unless the ion temperature is somewhat larger than 10 keV.

For $\bar{\eta}_{pe}^2 \ll 1$, the exponential does not rapidly damp large u values, and so the relevant piece of the integrand is that with $u \gg 1$ where

$$\psi\left(1+\frac{i}{u}\right)\simeq\psi(1)=-\gamma,$$
 (B12)

leading to

$$\begin{split} A_e^{\Delta Q}(\bar{\eta}_{pe}) &\simeq -\bar{\eta}_{pe}^2 \int_0^\infty du u \exp\left(-\frac{3}{2}\bar{\eta}_{pe}^2 u^2\right) (-2\gamma + \ln u^2) \\ &= \frac{1}{3} \ln\left(\frac{3}{2}\bar{\eta}_{pe}^2\right) + \gamma. \end{split} \tag{B13}$$

Adding this result to the classical limit (B2) gives the complete plasma electron contribution for a low energy projectile as follows:

$$E \ll T \bar{\eta}_{pe}^2 \ll 1:$$

$$\mathcal{A}_e(v_p) = \frac{e_p^2 \kappa_e^2}{4\pi} \left(\frac{\beta_e m_e}{2\pi}\right)^{1/2} \frac{v_p}{3} \left[\ln\left(\frac{8T_e m_{pe}^2}{m_e \hbar^2 \kappa_D^2}\right) - \gamma - 1 \right].$$
(B14)

For $\bar{\eta}_{pi}^2 \gg 1$, the exponential rapidly damps large u values, and so the relevant piece of the integrand is that with $u \ll 1$ where

$$\left[2\operatorname{Re}\psi\left(1+\frac{i}{u}\right)+\ln u^{2}\right]\simeq\frac{1}{6}u^{2},\tag{B15}$$

and, thus,

$$\bar{\eta}_{pi}^2 \gg 1 : A_i^{\Delta Q}(\bar{\eta}_{pi}) \simeq -\frac{\bar{\eta}_{pi}^2}{6} \int_0^\infty du \, u^3 \, \exp\left(-\frac{3}{2}\bar{\eta}_{pi}^2 \, u^2\right)$$

$$= -\frac{1}{27} \, \bar{\eta}_{pi}^{-2}. \tag{B16}$$

Since this is a very small correction to $A_i^c > 0$, it may be neglected, and we may use the pure classical limit (B2) for the ion contribution as follows:

$$E \ll T, \quad \bar{\eta}_{pi}^2 \gg 1 : \mathcal{A}_i(v_p) = \frac{e_p^2 \kappa_i^2}{4\pi} \left(\frac{\beta_i m_i}{2\pi}\right)^{1/2} \times \frac{2v_p}{3} \left[\ln\left(\frac{16\pi}{e_p e_i \beta_i \kappa_p} \frac{m_{pi}}{m_i}\right) - \frac{1}{2} - 2\gamma \right]. \quad (B17)$$

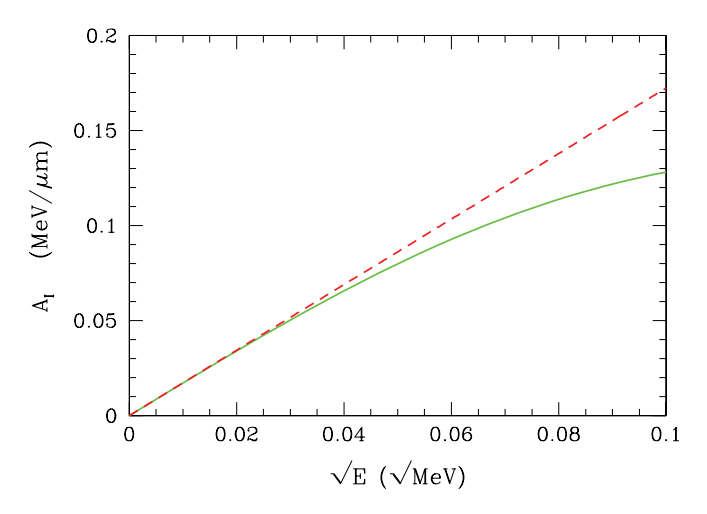


FIG. 8. (Color online) The ion contribution \mathcal{A}_I (solid) plotted with the corresponding low-energy approximate linear form (dashed) which is given by Eqs. (B17) and (B18). The plasma is equimolar DT with $T_e = T_1 = 10$ keV and $n_e = 1.0 \times 10^{25}$ cm⁻³, and the projectile is an α particle. For these parameters, the plasma coupling is $g_e = 0.0006$. Since the leading-order small-energy behavior is proportional to v_p , the graph of \mathcal{A}_1 against \sqrt{E} is linear in this region.

The total contribution of the ions in the plasma in this case is obviously

$$E \ll T$$
, $\bar{\eta}_{pi}^2 \gg 1$: $\mathcal{A}_{l}(v_p) = \sum_{i} \mathcal{A}_{i}(v_p)$. (B18)

In Figs. 8 and 9 we plot the ion and electron \mathcal{A} coefficients for an equimolar DT plasma with an electron density $n_e = 1.0 \times 10^{25} \, \mathrm{cm}^{-3}$ and equal electron and ion temperatures $T_e = T_1 = 10 \, \mathrm{keV}$ against the square root of the projectile energy \sqrt{E} . We make this choice because in the small-energy regime the coefficients are linear in the projectile velocity; therefore,

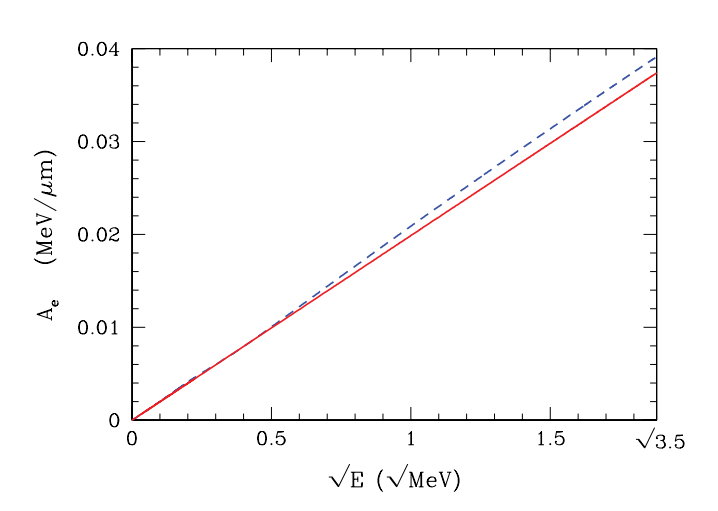


FIG. 9. (Color online) The electron contribution \mathcal{A}_e (solid) plotted with the corresponding low-energy approximate linear form (dashed) which is given by Eq. (B14). The plasma is the same as in the previous figure. Note that the linear approximation holds well into the DT fusion production energy of 3.54 MeV for the α particles.

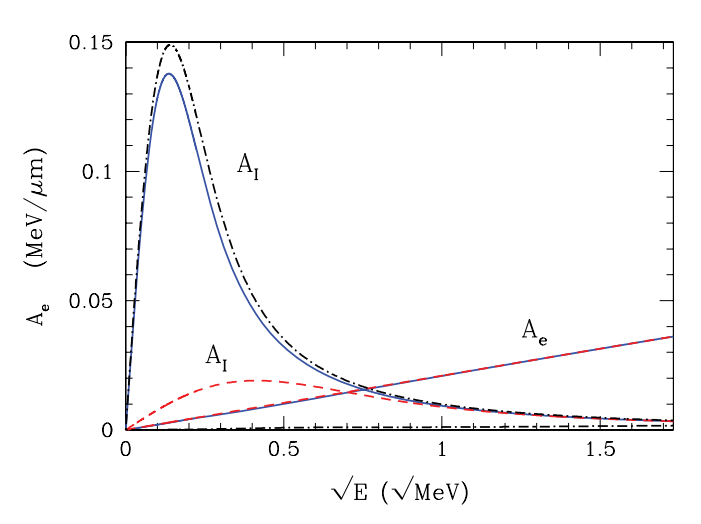


FIG. 10. (Color online) The coefficients \mathcal{A}_e and \mathcal{A}_I are plotted together for three different temperatures for an equimolar DT plasma with an electron number density $n_e = 1.0 \times 10^{25} \text{ cm}^{-3}$. The ion contributions \mathcal{A}_I peak to the left in the figure. The temperatures are (i) $T_e = 10 \text{ keV}$ and $T_I = 10 \text{ keV}$ (solid), (ii) $T_e = 10 \text{ keV}$ and $T_I = 10 \text{ keV}$ and $T_I = 10 \text{ keV}$ (dashed), (iii) $T_e = 100 \text{ keV}$ and $T_I = 10 \text{ keV}$ (dashed-dotted). The electron contributions \mathcal{A}_e for cases (i) and (ii) are almost equal, whereas for case (iii) \mathcal{A}_e is very small.

the graphs exhibit linear behavior until they start to depart from the low energy limit. 10

In Fig. 10 the coefficients A_e and A_I are plotted together for three different temperatures.

2. $E \gg T$: Total ionic contribution

For the total ionic contribution, it is convenient to first work out the regular part of the long-distance, dielectric contribution because it is the same for both cases of classical and quantum-mechanical scattering. With a trivial integration variable change, Eq. (A5) presents this contribution as

$$\mathcal{A}_{I,R}^{<}(v_p) = \frac{e_p^2}{4\pi} \, \frac{1}{v_p^2} \, \frac{i}{2\pi} \int_{-v_p}^{+v_p} dv \, v \, \frac{\rho_{I}(v)}{\rho_{total}(v)} \, F(v) \, \ln\left[\frac{F(v)}{K^2}\right], \tag{B19}$$

where we now write

$$\rho_{\rm I}(v) = \sum_{i} \rho_{i}(v) \tag{B20}$$

so

$$\rho_{\text{total}}(v) = \rho_e(v) + \rho_{\text{I}}(v), \tag{B21}$$

¹⁰Figures 8 and 9, for $n_e = 1.0 \times 10^{25}$ cm⁻³ and $T_e = T_1 = 10$ keV, show that A_1 departs from the linear approximation at about $\sqrt{E} = 0.04 \sqrt{\text{MeV}}$ while A_e departs from linearity at about $\sqrt{E} = 0.80 \sqrt{\text{MeV}}$. Curves for the same electron density but for $T_e = 10$ keV, $T_1 = 100$ keV and $T_e = 100$ keV, $T_1 = 10$ keV have the same general shape as the curves in Figs. 8 and 9, but the corresponding regions of validity for the linear approximation change to $\sqrt{E} = 0.12 \sqrt{\text{MeV}}$, $\sqrt{E} = 0.04 \sqrt{\text{MeV}}$ for A_1 while for A_e the corresponding numbers are $\sqrt{E} = \sqrt{3.5} \sqrt{\text{MeV}} = 1.87 \sqrt{\text{MeV}}$, $\sqrt{E} = 0.16 \sqrt{\text{MeV}}$.

with the weight functions ρ given by Eq. (A7). Assuming that the charges of the ions do not differ greatly from the charge of the electron, then $\kappa_e^2/\kappa_1^2 \simeq T_1/T_e$ and the integrand of Eq. (B19) involves a factor that has the behavior

$$\frac{\rho_{\rm I}(v)}{\rho_{\rm total}(v)} = \frac{1}{1 + \rho_e(v)/\rho_{\rm I}(v)}$$

$$\simeq \frac{1}{1 + \left(m_e T_{\rm I}^3/m_1 T_e^3\right)^{1/2} \exp(m_1 v^2/2T_{\rm I})}, \quad (B22)$$

where $m_{\text{\tiny I}}$ is a typical ion mass. Thus, defining a typical ionic thermal velocity $v_{\text{\tiny T}}$ by

$$m_{\scriptscriptstyle \rm I} v_{\scriptscriptstyle \rm T}^2 = T_{\scriptscriptstyle \rm I}, \tag{B23}$$

this factor remains unity up to the critical velocity $v_{\rm crit}$ defined by

$$v_{\text{crit}}^2 = v_{\text{T}}^2 \ln \left(\frac{m_1 T_e^3}{m_e T_1^3} \right),$$
 (B24)

after which it falls fairly rapidly to zero. The logarithmic factor in Eq. (B24) is typically about a factor of 10. So $v_{\rm crit}$ is somewhat larger than an ion thermal velocity yet it is considerably smaller than the electron thermal velocity.

In this region in which the factor $\rho_{\rm t}(v)/\rho_{\rm total}(v)$ of the integrand is nonvanishing, the function [Eq. (A9) above]

$$F(v) = -\int_{-\infty}^{+\infty} du \frac{\rho_{\text{total}}(u)}{v - u + i\eta}$$
 (B25)

has the form

$$F(v) = \tilde{F}(v) = \kappa_e^2 + F_{\rm I}(v), \tag{B26}$$

where

$$F_{\rm I}(v) = -\int_{-\infty}^{+\infty} du \frac{\rho_{\rm I}(u)}{v - u + i\,\eta}.\tag{B27}$$

This is so because the velocity v, which must be less than $v_{\rm crit}$, is much less than the electron thermal velocity. Hence, the electron part of F(v) takes on its low velocity limit, the electron Debye wave number squared κ_e^2 . We place the form (B26) into Eq. (B19) to obtain

$$\mathcal{A}_{\scriptscriptstyle I,R}^{\scriptscriptstyle <}(v_p) \simeq \frac{e_p^2}{4\pi} \, \frac{1}{v_p^2} \, \frac{i}{2\pi} \int_{-v_p}^{+v_p} dv \, v \, \frac{\rho_{\scriptscriptstyle I}(v)}{\rho_{\scriptscriptstyle total}(v)} \, \tilde{F}(v) \, \ln\left[\frac{\tilde{F}(v)}{\kappa_e^2}\right]. \tag{B28}$$

Here we have replaced the arbitrary intermediate wave number K by the electron Debye wave number κ_e because then

$$v \to \infty : \frac{\tilde{F}(v)}{\kappa_e^2} \to 1 - \frac{\omega_{\rm I}^2}{\kappa_e^2 v^2},$$
 (B29)

where

$$\omega_{\rm I}^2 = \sum_i \omega_i^2 = \sum_i \frac{e_i^2 n_i}{m_i},$$
 (B30)

and so $\ln(\tilde{F}(v)/\kappa_e^2)$ vanishes for large v. In order of magnitude,

$$\frac{\omega_{_{\rm I}}^2}{\kappa^2 v^2} \simeq \frac{T_e}{m_{_{\rm T}} v^2} = \frac{T_e}{T_{_{\rm T}}} \frac{v_{_{\rm T}}^2}{v^2}.$$
 (B31)

Hence, since $v_{\rm T}^2$ is much less than $v_{\rm crit}^2$, unless T_e is considerably larger than $T_{\rm I}$, the final factor in the integral (B28), $\ln(\tilde{F}(v)/\kappa_e^2)$, vanishes before $\rho_{\rm I}(v)/\rho_{\rm total}(v)$ departs significantly from unity. Hence, we simply take $\rho_{\rm I}(v)/\rho_{\rm total}(v)=1$ and write

$$\mathcal{A}_{1,R}^{<}(E_p) \simeq \frac{e_p^2}{4\pi} \frac{1}{v_p^2} \frac{i}{2\pi} \int_{-v_p}^{+v_p} dv \, v \, \tilde{F}(v) \, \ln\left[\frac{\tilde{F}(v)}{\kappa_e^2}\right].$$
 (B32)

The discussion above shows that when $v_p > v_{\rm crit}$, the limits of the integration may be replaced by $\pm \infty$. Recalling the definition (B24) of the critical velocity $v_{\rm crit}$, and assuming that the projectile mass m_p is about the same as the typical ion mass m_1 in the plasma, we can now state that

$$E > T \ln\left(\frac{m_1 T_e^3}{m_e T_1^3}\right) : \mathcal{A}_{l,R}^{<}(E_p)$$

$$= \frac{e_p^2}{4\pi} \frac{1}{v_p^2} \frac{i}{2\pi} \int_{-\infty}^{+\infty} dv \, v \, \tilde{F}(v) \ln\left[\frac{\tilde{F}(v)}{\kappa_e^2}\right]. \quad (B33)$$

We should note the convergence of the integral requires that the integration limits are to be taken in a rigorously symmetrical fashion with the integral performed between exactly $-v_p$ and $+v_p$ and then $v_p \to \infty$ taken. It is now a simple matter to evaluate this limiting form. Adding a semicircle in the upper half plane of radius v_p gives a closed contour integral with no interior singularities that accordingly vanishes. Hence, the value of the original integral is the negative of the integral over this large semicircle, an integral that is trivially performed using the limiting forms listed before. Thus,

$$E > T \ln \left(\frac{m_1 T_e^3}{m_e T_i^3} \right) : \mathcal{A}_{I,R}^{<}(v_p) = -\frac{e_p^2}{4\pi} \frac{\omega_i^2}{2 v_p^2}.$$
 (B34)

With the long-distance, dielectric ionic contribution evaluated in the projectile high energy limit, we can now compute the complete function $\mathcal{A}_i(v_p)$ in this limit. To do so, we must distinguish two cases for the remaining hard scattering contribution.

a.
$$E \gg T$$
, $\eta_{ni}^2 \gg 1$

As shown in detail in Sec. 10 of BPS, the classical scattering contribution dominates when the Coulomb parameter η_{pi} is large, with the first quantum-mechanical correction of relative order

$$\eta_{pi}^{-2} = \left(\frac{4\pi\hbar v_p}{e_p e_i}\right)^2 = \left(\frac{e^2}{e_p e_i}\right)^2 \frac{2E}{\alpha^2 m_p c^2},$$
(B35)

where $\alpha \simeq 1/137$ is the fine structure constant. In this classical limit, the scattering contribution is given by Eq. (A3). For the previous evaluation of the dielectric contribution to hold, we must choose $K = \kappa_e$ so this formula reads

$$\mathcal{A}_{i,s}^{c}(v_{p}) = \frac{e_{p}^{2} \kappa_{i}^{2}}{4\pi} \left(\frac{\beta_{i} m_{i}}{2\pi} \right)^{1/2} v_{p} \int_{0}^{1} du u^{1/2} \exp\left(-\frac{1}{2} \beta_{i} m_{i} v_{p}^{2} u \right) \times \left[-\ln\left(\beta_{i} \frac{e_{p} e_{i}}{4\pi} \kappa_{e} \frac{m_{i}}{m_{pi}} \frac{u}{1-u} \right) - 2\gamma + 2 \right].$$
(B36)

Since $m_i v_p^2 / 2 \sim E \gg T_i$, only small u values are significant. Hence, we can approximate 1 - u = 1 within the logarithm

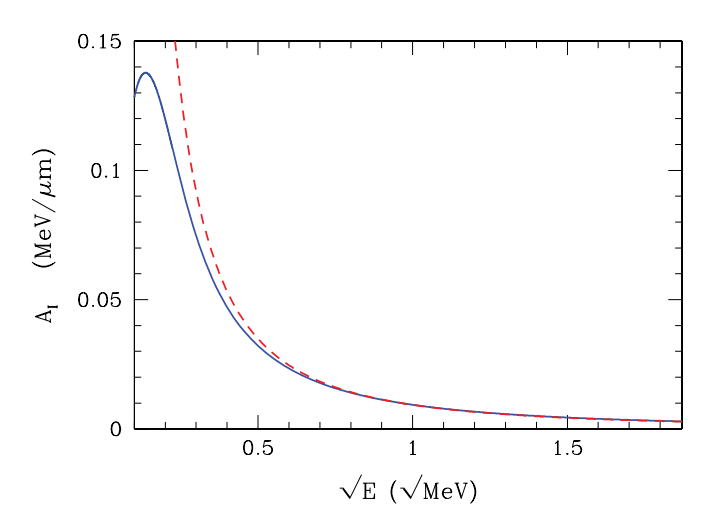


FIG. 11. (Color online) $A_{\rm I}$ (solid curve) vs. its large-energy (dashed curve) asymptotic form. The plasma is equimolar DT with $n_e = 1.0 \times 10^{25} {\rm cm}^{-3}$ and $T_e = T_{\rm I} = 10 {\rm keV}$.

and extend the integration limit to $u \to \infty$. With the variable change $(\beta_i m_i v_p^2/2) u = s^2$, we obtain the high energy limit

$$\mathcal{A}_{i,s}^{c}(v_{p}) = \frac{e_{p}^{2}}{4\pi} \frac{\omega_{i}^{2}}{v_{p}^{2}} \frac{4}{\sqrt{\pi}} \int_{0}^{\infty} ds \, s^{2} \exp(-s^{2})$$

$$\times \left[\ln \left(\frac{4\pi}{e_{p}e_{i}\kappa_{e}} \frac{m_{pi}v_{p}^{2}}{2} \right) - \ln s^{2} - 2\gamma + 2 \right], \tag{B37}$$

where we have used $\kappa_i^2/\beta_i m_i = \omega_i^2$. Here we have the integrals

$$\frac{4}{\sqrt{\pi}} \int_0^\infty ds \, s^2 \exp(-s^2) = 1$$
 (B38)

and

$$\frac{4}{\sqrt{\pi}} \int_0^\infty ds \, s^2 \exp(-s^2) \ln s^2$$

$$= \frac{2}{\sqrt{\pi}} \Gamma\left(\frac{3}{2}\right) \psi\left(\frac{3}{2}\right) = \psi\left(\frac{3}{2}\right) = 2 - \gamma - \ln 4. \quad (B39)$$

Whence,

$$\mathcal{A}_{i,s}^{c}(v_{p}) = \frac{e_{p}^{2}}{4\pi} \frac{\omega_{i}^{2}}{v_{p}^{2}} \left[\ln \left(\frac{16\pi}{e_{p}e_{i}\kappa_{e}} \frac{m_{pi}v_{p}^{2}}{2} \right) - \gamma \right], \quad (B40)$$

which, summed over all the ions in the plasma and combined with the previous long-distance result, (B34) yields the total contribution from the ions in the plasma:

$$E \gg T, \quad \eta_{pi}^2 \gg 1:$$

$$\mathcal{A}_{I}(v_p) = \sum_{i} \mathcal{A}_{i}(v_p) = \sum_{i} \left[\mathcal{A}_{i,s}^{c}(v_p) + \mathcal{A}_{i,R}^{c}(v_p) \right]$$

$$= \frac{e_p^2}{4\pi} \frac{1}{v_p^2} \sum_{i} \omega_i^2 \left[\ln \left(\frac{16\pi}{e_p e_i \kappa_e} \frac{m_{pi} v_p^2}{2} \right) - \gamma - \frac{1}{2} \right].$$
(B41)

See Fig. 11 for a comparison of A_i with its asymptotic form at large energy.

b.
$$E \gg T$$
, $\eta_{ni}^2 \ll 1$

In this case, we have the limit

$$v_{p} \to \infty : \mathcal{A}_{i,s}^{c}(v_{p}) + \mathcal{A}_{i}^{\Delta Q}(v_{p})$$

$$= \frac{e_{p}^{2}}{4\pi} \frac{1}{v_{p}^{2}} \sum_{i} \omega_{i}^{2} \ln \left(\frac{2m_{pi}v_{p}}{\hbar \kappa_{e}}\right), \tag{B42}$$

which is contained in Eq. (10.42) of BPS. Adding this result to Eq. (B34) now provides the complete $v_p \to \infty$ limit for the ion part of the \mathcal{A}_1 coefficient:

$$E \gg T, \quad \eta_{pi}^2 \ll 1 : \mathcal{A}_{\mathsf{I}}(v_p)$$

$$= \frac{e_p^2}{4\pi} \frac{1}{v_p^2} \sum_{i} \omega_i^2 \left[\ln \left(\frac{2m_{pi} v_p}{\hbar \kappa_e} \right) - \frac{1}{2} \right]. \tag{B43}$$

3. $T \ll E \ll m_p T/m_e$: Electronic contribution

There is an intermediate range of projectile energies in which the projectile energy is much larger that the temperature, $E \gg T$, but yet not so large that we have $E \ll (m_p/m_e) T \sim 10^4 T$. We examine this range here.

We again need to work out its long-distance, dielectric contribution, and its short-distance scattering contribution.

a. Dielectric part

In the energy range specified, the typical velocity in the dielectric function is small in comparison with the electron average thermal velocity and large in comparison with an ion average thermal velocity. Hence, in this range,

$$F(v) \simeq \kappa_e^2 - \frac{\omega_{\rm I}^2}{v^2} + \pi i \,\rho_{\rm total}(v). \tag{B44}$$

Here, in the dominant integration range,

$$\frac{\omega_{\rm I}^2}{\kappa_{\rm e}^2 v^2} \simeq \frac{T}{m_{\rm I} v^2} \ll 1,\tag{B45}$$

and so we may simply write

$$F(v) \simeq \kappa_e^2 + \pi i \ \rho_{\text{total}}(v).$$
 (B46)

Moreover, in the dominant integration range, the imaginary part π $\rho_{\text{total}}(v)$ is small in comparison to κ_e^2 . Writing Eq. (A5) as

$$\mathcal{A}_{e,R}^{<}(v_p) \simeq \frac{e_p^2}{4\pi} \frac{i}{2\pi} \int_0^1 d\cos\theta \cos\theta \frac{\rho_e(v_p\cos\theta)}{\rho_{\text{total}}(v_p\cos\theta)} \times \frac{1}{2} \left\{ [F(v_p\cos\theta) - F(-v_p\cos\theta)] \right. \\ \times \ln \left[\frac{F(v_p\cos\theta)F(-v_p\cos\theta)}{K^4} \right] \\ + [F(v_p\cos\theta) + F(-v_p\cos\theta)] \\ \times \ln \left[\frac{F(v_p\cos\theta)}{F(-v_p\cos\theta)} \right] \right\}, \tag{B47}$$

and using Eq. (B46) with the imaginary part treated to first order,

$$\mathcal{A}_{e,R}^{<}(v_p) \simeq -\frac{e_p^2}{4\pi} \int_0^1 d\cos\theta \, \cos\theta \, \rho_e(v_p \cos\theta) \left[\ln\left(\frac{\kappa_e^2}{K^2}\right) + 1 \right].$$
(B48)

In our energy range Eq. (A7) becomes

$$\rho_e(v) = \kappa_e^2 \sqrt{\frac{\beta_e m_e}{2\pi}} v, \tag{B49}$$

and so

$$\mathcal{A}_{e,R}^{<}(v_p) \simeq -\frac{e_p^2}{4\pi} \,\kappa_e^2 \,\sqrt{\frac{\beta_e m_e}{2\pi}} \,v_p \,\frac{1}{3} \left[\ln\left(\frac{\kappa_e^2}{K^2}\right) + 1 \right].$$
 (B50)

b. Scattering part

The electrons in the hot plasmas that we consider have such large velocities that their scattering off the projectiles is quantum mechanical. This is described by Eq. (10.41) of BPS which gives

$$\eta_{pe} \to 0: \mathcal{A}_{e,s}^{c}(v_{p}) + \mathcal{A}_{e}^{\Delta Q}(v_{p})
= \frac{e_{p}^{2} \kappa_{e}^{2}}{4\pi} \left(\frac{\beta_{e} m_{e}}{2\pi}\right)^{1/2} v_{p} \int_{0}^{1} du \, u^{1/2} \exp\left(-\frac{1}{2} \beta_{e} m_{e} v_{p}^{2} u\right)
\times \frac{1}{2} \left[-\ln\left(\frac{\beta_{e} \hbar^{2} K^{2}}{2m_{pe}} \frac{m_{e}}{m_{pe}} \frac{u}{1-u}\right) - \gamma + 2\right].$$
(B51)

With $E = \frac{1}{2} m_p v_p^2 \ll m_p T/m_e$, the damping constant in the exponent $\beta_e m_e v_p^2/2$ is now small, not large as it was before. Hence, the exponential may simply be replaced by unity, and we encounter the integrals

$$\int_0^1 du \, u^{1/2} = \frac{2}{3},\tag{B52}$$

and

$$\int_0^1 du \, u^{1/2} \ln \left(\frac{u}{1 - u} \right) = \frac{2}{3} \, (2 - \ln 4) \,. \tag{B53}$$

Hence.

$$\mathcal{A}_{e,s}^{c}(v_{p}) + \mathcal{A}_{e}^{\Delta Q}(v_{p}) = \frac{e_{p}^{2} \kappa_{e}^{2}}{4\pi} \left(\frac{\beta_{e} m_{e}}{2\pi}\right)^{1/2} v_{p} \frac{1}{3} \left[\ln \left(\frac{8T_{e} m_{pe}^{2}}{m_{e} \hbar^{2} K^{2}}\right) - \gamma \right]. \quad (B54)$$

c. The sum

The sum of the dielectric part (B50) and the scattering part (B54) gives

$$E \gg T, \quad m_e E/m_p \ll T : \text{or } T \ll E \ll \frac{m_p}{m_e} T :$$

$$\mathcal{A}_e(v_p) \simeq \frac{e_p^2 \kappa_e^2}{4\pi} \left(\frac{\beta_e m_e}{2\pi}\right)^{1/2} \frac{v_p}{3} \left[\ln \left(\frac{8T_e m_{pe}^2}{m_e \hbar^2 \kappa_e^2}\right) - \gamma - 1 \right]. \tag{B55}$$

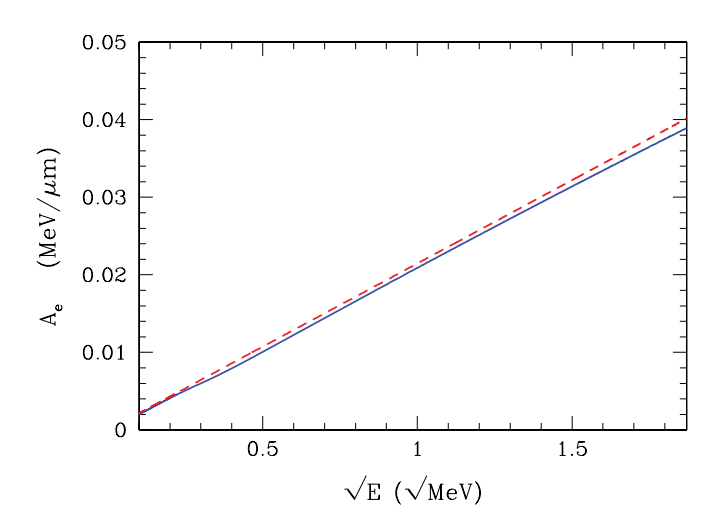


FIG. 12. (Color online) The coefficient A_e (solid curve) compared with the high-energy (dashed curve) approximation (B55). The plasma is equimolar DT with $n_e = 1.0 \times 10^{25}$ cm⁻³ and $T_e = T_1 = 10$ keV.

Figure 12 compares this high-energy approximation with the exact result. Figure 13 shows that the high- and low-energy approximations are quite similar.

4. $E \gg m_p T/m_e$: Electronic contribution

The high velocity limit in this case has already been calculated by BPS in Eq. (10.43), which we simply quote here,

$$v_p \to \infty$$
: $\mathcal{A}_e(v_p) = \frac{e_p^2}{4\pi} \frac{\omega_e^2}{v_p^2} \ln\left(\frac{2m_{pe}v_p^2}{\hbar\omega_e}\right)$. (B56)

This limit is mostly academic, since the system enters the relativistic regime at these high velocities.

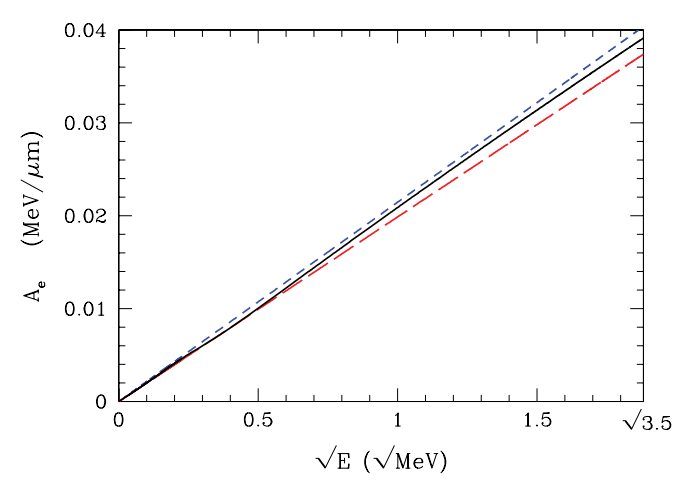


FIG. 13. (Color online) An α -particle projectile moving in an equimolar DT plasma with $T_e = T_1 = 10$ keV and $n_e = 1.0 \times 10^{25}$ cm⁻³. The low-energy approximation (B14) (short-dashed curve) lies above the exact result (solid curve) while the high-energy approximation (B55) (long-dashed curve) lies below the exact result (solid curve). Because $\kappa_D^2 = 2\kappa_e^2$ for our equimolar DT plasma, the two approximate forms (B14) and (B55) differ only by a factor of 2 inside the logarithm, and this leads to only slightly different slopes.

5. Energy crossover

As we have made explicit, the energy loss to the ions in the plasma dominates at low projectile energies while the loss is to the electrons at high projectile energies. Here we shall estimate the crossover point, the projectile energy at which the two types of loss mechanisms are comparable. We shall find that this occurs at a projectile energy that is much greater than a typical plasma temperature T, and so we will assume the limit $E \gg T$ in estimating the crossover point.

For the ions, the $E \gg T$ result (B41) reads

$$\mathcal{A}_{I}(v_{p}) = \frac{e_{p}^{2}}{4\pi} \sum_{i} \frac{\omega_{i}^{2}}{v_{p}^{2}} \left[\ln \left(\frac{16\pi}{e_{p}e_{i}\kappa_{e}} \frac{m_{pi}v_{p}^{2}}{2} \right) - \gamma - \frac{1}{2} \right]. \tag{B57}$$

This holds provided that

$$\eta_{pi}^{-2} = \left(\frac{4\pi\hbar v_p}{e_p e_i}\right)^2 = \left(\frac{e^2}{e_p e_i}\right)^2 \frac{2E}{\alpha^2 m_p c^2} \ll 1.$$
 (B58)

To put the total ion contribution in a convenient form, replace the ion charge e_i inside the logarithm of Eq. (B57) by a typical value e_I , approximate $m_{pi} \approx m_p/2$, and define

$$\sum_{i} \omega_i^2 = \omega_{\rm I}^2, \tag{B59}$$

where we replace the ion charge e_i inside the logarithm by a typical value e_1 and write $m_{pi} \simeq m_p/2$ to approximate the total ion contribution by

$$\mathcal{A}_{\rm I}(v_p) \simeq \frac{e_p^2}{4\pi} \frac{\omega_{\rm I}^2}{v_p^2} \left[\ln \left(\frac{8\pi}{e_p e_{\rm I} \kappa_e} E \right) - \gamma - \frac{1}{2} \right]. \tag{B60}$$

Note that the only temperature dependence in this result is within the electron Debye wave number inside the logarithm. Hence, the result only weakly depends on the plasma temperatures.

A reasonably good approximation for the crossover projectile speed $v_p = v_c$ should be obtained by equating the ion result (B60) to the electronic result (B55) which we repeat here using $\kappa_e^2 = \beta_e m_e \, \omega_e^2$:

$$\mathcal{A}_{e}(v_{p}) = \frac{e_{p}^{2}}{4\pi} \frac{\omega_{e}^{2}}{3} \left(\frac{2}{\pi}\right)^{1/2} \left(\frac{m_{e}}{T_{e}}\right)^{3/2} \times v_{p} \left[\ln\left(\frac{\sqrt{8T_{e}m_{e}}}{\hbar\kappa_{e}}\right) - \frac{1}{2}(\gamma + 1)\right]. \quad (B61)$$

In equating the ion and electron approximations (B60) and (B61) we use the crossover energy defined by

$$E_{\rm c} = \frac{1}{2} m_p v_{\rm c}^2 \tag{B62}$$

to obtain

$$E_{c}^{3/2} \left[\ln \left(\frac{\sqrt{8T_{e}m_{e}}}{\hbar \kappa_{e}} \right) - \frac{1}{2} (\gamma + 1) \right]$$

$$= T_{e}^{3/2} \left(\frac{9\pi}{16} \right)^{3/2} \left(\frac{m_{p}}{m_{e}} \right)^{3/2} \frac{\omega_{r}^{2}}{\omega_{e}^{2}} \left[\ln \left(\frac{8\pi E_{c}}{e_{p}e_{1}\kappa_{e}} \right) - \gamma - \frac{1}{2} \right].$$
(B63)

It is important to note that this crossover point only depends on the electron temperature T_e . The ion temperature T_I is of no relevance here.

Note that the results that we have obtained provide an approximate form for the total \mathcal{A} coefficient as a function of the energy $E = m_p v_p^2/2$, $\mathcal{A}(E) = \mathcal{A}_e(E) + \mathcal{A}_i(E)$, namely

$$\mathcal{A}(E) = \lambda E^{1/2} \left[1 + \left(\frac{E_{\rm c}}{E} \right)^{3/2} \right], \tag{B64}$$

where

$$\lambda = \frac{e_p^2}{4\pi} \frac{\omega_e^2}{3} \left(\frac{1}{\pi}\right)^{1/2} \left(\frac{m_e}{T_c}\right)^{3/2} \frac{2}{m_p^{1/2}} \times \left[\ln\left(\frac{\sqrt{8T_e m_e}}{\hbar \kappa_e}\right) - \frac{1}{2}(\gamma + 1)\right]. \tag{B65}$$

To return to assess the validity of our approximation for the crossover energy, we examine equimolar DT plasmas traversed by α particles of mass $m_p = m_\alpha$, charge $e_p = 2e$, and initial energy $E_0 = 3.54$ MeV produced by DT fusion. In numerical terms for this case with the electron temperature T_e and the crossover energy E_c measured in keV, and the electron number density n_e measured in cm⁻³, the crossover relation (B63) appears as

$$E_{c}^{3/2} \left[\ln \left(5.796 \times 10^{27} \frac{T_{e}^{2}}{n_{e}} \right) - 1.577 \right]$$

$$= 188.1 \ T_{e}^{3/2} \left[\ln \left(2.66 \times 10^{28} \frac{T_{e}}{n_{e}} E_{c}^{2} \right) - 2.154 \right].$$
(B66)

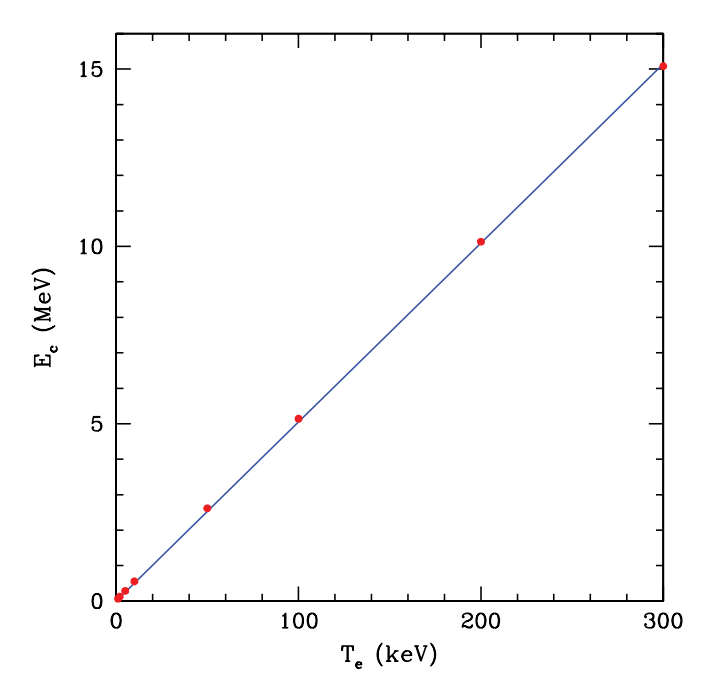


FIG. 14. (Color online) Solutions (dots) of the crossover condition (B66) as a function of the electron temperature for an electron number density $n_e = 1.0 \times 10^{25} \text{ cm}^{-3}$. The straight line is a fit to these points, with $E_C = 51 T_e$. Similar results obtain for the other densities, with the results presented in Eq. (B67).

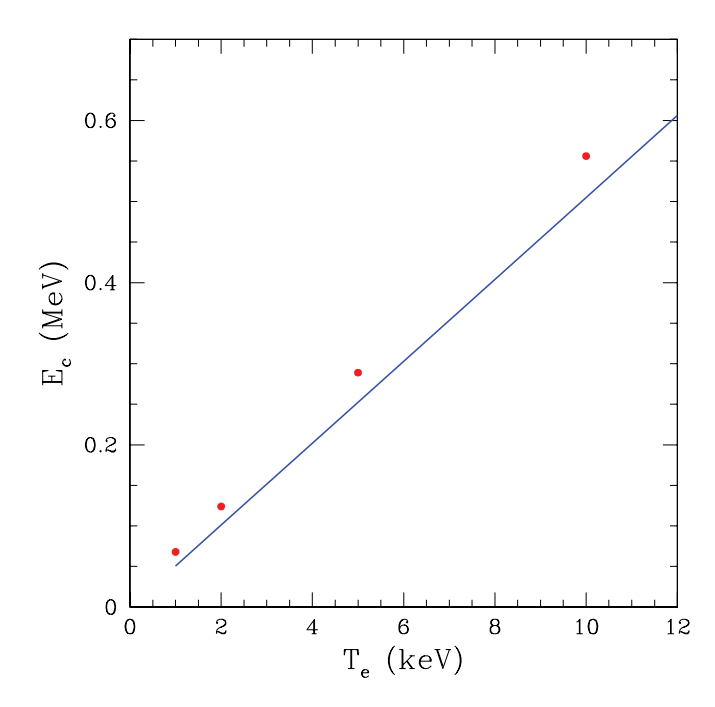


FIG. 15. (Color online) This figure displays the lower temperature region of the previous Fig. 14. Here the linear relation can deviate from the points which are solutions of the crossover relation (B66) with an error on the order of 10%.

We find that the crossover energies for different electron densities n_e are nearly linear functions of T_e given by

$$E_{\rm c} \simeq T_e \begin{cases} 48 \,, & n_e = 1.0 \times 10^{24} \,\mathrm{cm}^{-3}, \\ 51 \,, & n_e = 1.0 \times 10^{25} \,\mathrm{cm}^{-3}, \\ 53 \,, & n_e = 1.0 \times 10^{26} \,\mathrm{cm}^{-3}. \end{cases}$$
(B67)

The linear fit for $n_e = 1.0 \times 10^{25} \, \mathrm{cm}^{-3}$ is displayed in Fig. 14. Figure 15 shows that for energies below 10 keV or so, these linear relations break down by about 10%.

APPENDIX C: THE G FUNCTION SIMPLIFIED

Here we turn to the definition (4.29) of $G(T_1, T_e; E_0)$ in order to reduce it to a more manageable form. For convenience, we repeat this definition here¹¹ as follows:

$$G(T_1, T_e; E_0) = \int_0^\infty dE \ F(E) e^{-S(E)} \int_0^E \frac{dE'}{E'} \frac{e^{+S(E')}}{\langle T \mathcal{A}(E') \rangle} \times \left[\theta(E_0 - E') - \int_{E'}^\infty dE'' \sqrt{E''} \overline{\mathcal{N}} e^{-S(E'')} \right],$$
(C1)

¹¹We recall that G gives a contribution

$$\frac{\Delta E_{\rm I}}{E_0} = \left(\frac{T_e - T_{\rm I}}{E_0}\right) G(T_{\rm I}, T_e; E_0).$$

Since the prefactor multiplying G involves a temperature difference that is at most 300 keV and the energy E_0 is typically 3.5 MeV, this prefactor is less than about 9%. Hence, to within an accuracy of a few tenths of a percentage, we need only compute the pure number G to an absolute precision of 0.1.

where

$$\overline{\mathcal{N}}^{-1} = \int_0^\infty dE' \sqrt{E'} e^{-S(E')}, \tag{C2}$$

and

$$F(E) = E \frac{\mathcal{A}_{I}(E)\mathcal{A}_{e}(E)}{\langle T\mathcal{A}(E)\rangle}.$$
 (C3)

First, we note that if $E' < E_0$, the θ function in the square brackets is unity. Hence, we can make use of the sum rule (4.7) to write

$$G(T_1, T_e; E_0)$$
= $G_1(T_1, T_e; E_0) + G_2(T_1, T_e; E_0) + G_3(T_1, T_e; E_0)$, (C4)

where

$$G_{1}(T_{1}, T_{e}; E_{0}) = \int_{0}^{E_{0}} dE \ F(E) e^{-S(E)} \int_{0}^{E} \frac{dE'}{E'} \frac{e^{+S(E')}}{\langle T \mathcal{A}(E') \rangle} \times \int_{0}^{E'} dE'' \sqrt{E''} \ \overline{\mathcal{N}} e^{-S(E'')}, \tag{C5}$$

$$G_{2}(T_{1}, T_{e}; E_{0}) = \int_{E_{0}}^{\infty} dE \ F(E) e^{-S(E)} \int_{0}^{E_{0}} \frac{dE'}{E'} \frac{e^{+S(E')}}{\langle T \mathcal{A}(E') \rangle} \times \int_{0}^{E'} dE'' \sqrt{E''} \ \overline{\mathcal{N}} e^{-S(E'')}, \tag{C6}$$

and

$$G_{3}(T_{1}, T_{e}; E_{0}) = -\int_{E_{0}}^{\infty} dE \ F(E) e^{-S(E)} \int_{E_{0}}^{E} \frac{dE'}{E'} \frac{e^{+S(E')}}{\langle T \mathcal{A}(E') \rangle} \times \int_{E'}^{\infty} dE'' \sqrt{E''} \ \overline{\mathcal{N}} e^{-S(E'')}.$$
(C7)

First, we show that G_3 may be neglected. For the very last pair of integrals in G_3 , since the energies E' and E'' are larger than $E_0 \gg T_e$, T_1 , the electron contribution to the \mathcal{A}_b functions dominate, and so

$$S(E'') - S(E') = \frac{1}{T_e} (E'' - E').$$
 (C8)

This is a very large number unless E'' is near E'. Hence, with corrections that will be of the very small order T_e/E_0 , we have

$$\int_{E_{0}}^{E} \frac{dE'}{E'} \frac{e^{+S(E')}}{\langle T\mathcal{A}(E')\rangle} \int_{E'}^{\infty} dE'' \sqrt{E''} \, \overline{\mathcal{N}} e^{-S(E'')}$$

$$\simeq \int_{E_{0}}^{E} \frac{dE'}{E'} \frac{1}{T_{e}\mathcal{A}_{e}(E')} \sqrt{E'} \, \overline{\mathcal{N}} \int_{E'}^{\infty} dE''$$

$$\times \exp\left[-\frac{1}{T_{e}} \left(E'' - E'\right)\right] = \overline{\mathcal{N}} \int_{E_{0}}^{E} \frac{dE'}{\sqrt{E'}} \frac{1}{\mathcal{A}_{e}(E')},$$
(C9)

and so, again, since the electrons dominate the A_b functions in the high-energy regions that appear here,

$$G_3(T_1, T_e; E_0) \simeq -\int_{E_0}^{\infty} dE \, \frac{E}{T_e} \, \mathcal{A}_{\mathsf{I}}(E) \, e^{-S(E)} \, \overline{\mathcal{N}} \, \int_{E_0}^{E} \frac{dE'}{\sqrt{E'}} \, \frac{1}{\mathcal{A}_e(E')}. \tag{C10}$$

There is really no need to go any further in the evaluation of $G_3(T_1, T_e; E_0)$ since it has the exponentially small factor $\exp[-S(E)]$, with $E \ge E_0$. In this region, as we have noted, the electrons dominate and so $\exp[-S(E)] \simeq \exp(-E/T_e)$. Even for an electron temperature as high as 35 keV and for a DT fusion α particle with $E_0 = 3.54$ MeV, this factor is $\exp(-100) \simeq 4 \times 10^{-44}$.

For the evaluation of G_2 , it is convenient to define

$$H(E') = \int_0^{E'} dE'' \sqrt{E''} \, \overline{\mathcal{N}} \, e^{-S(E'')}. \tag{C11}$$

To isolate the leading pieces, we shall write

$$e^{\pm S(E)} = \pm \frac{\langle T \mathcal{A}(E) \rangle}{\mathcal{A}(E)} \frac{d}{dE} e^{\pm S(E)}$$
 (C12)

and integrate by parts. This will provide an extra explicit factor of a plasma temperature T in the numerator, thereby yielding a small quantity.

The final double integral in the triple integral (C6) defining G_2 now appears as

$$\int_{0}^{E_{0}} \frac{dE'}{E'} \frac{e^{+S(E')}}{\langle T \mathcal{A}(E') \rangle} \int_{0}^{E'} dE'' \sqrt{E''} \, \overline{\mathcal{N}} \, e^{-S(E'')} = \int_{0}^{E_{0}} dE' \, \frac{H(E')}{E' \mathcal{A}(E')} \frac{d}{dE'} \, e^{+S(E')} \\
\simeq \frac{H(E_{0})}{E_{0} \mathcal{A}(E_{0})} \, e^{+S(E_{0})} - \int_{0}^{E_{0}} dE' \, e^{+S(E')} \frac{d}{dE'} \left[\frac{H(E')}{E' \mathcal{A}(E')} \right] \\
\simeq \frac{H(E_{0})}{E_{0} \mathcal{A}(E_{0})} \, e^{+S(E_{0})} - \frac{\langle T \mathcal{A}(E_{0}) \rangle}{\mathcal{A}(E_{0})} \, e^{+S(E_{0})} \, \frac{d}{dE} \left[\frac{H(E)}{E \mathcal{A}(E)} \right]_{E_{0}} + \cdots, \quad (C13)$$

where the ellipsis represents the series resulting by further partial integrations. As we shall see, the second term in the last line of Eq. (C13) is already negligible and so are these omitted terms. The approximate equalities in Eq. (C13) neglect lower limit terms since they result in exponentially small quantities from the remaining integration over E in Eq. (C6) because of the factor $\exp[-S(E)]$ with $E > E_0$. Here, to very good accuracy,

$$H(E_0) = 1, (C14)$$

since the integral defining H(E) has long since converged to its limiting value at $E=E_0$. Hence,

$$\int_{0}^{E_{0}} \frac{dE'}{E'} \frac{e^{+S(E')}}{\langle T\mathcal{A}(E')\rangle} \int_{0}^{E'} dE'' \sqrt{E''} \overline{\mathcal{N}} e^{-S(E'')} \simeq \frac{1}{E_{0} \mathcal{A}(E_{0})} e^{+S(E_{0})} \left\{ 1 - \langle T\mathcal{A}(E)\rangle E \frac{d}{dE} \left[\frac{1}{E \mathcal{A}(E)} \right] \right|_{E_{0}} \right\}. \tag{C15}$$

Here, since at large energies the rate of energy variation is of order 1/E,

$$\langle T\mathcal{A}(E)\rangle E \frac{d}{dE} \left[\frac{1}{E\mathcal{A}(E)}\right]\Big|_{E_0} \sim \frac{\langle T\mathcal{A}(E_0)\rangle}{E_0\mathcal{A}(E_0)} \sim \frac{T}{E_0},$$
 (C16)

in which T is a typical plasma temperature. The ratio T/E_0 is at most a few percentages for the plasma parameters that we consider, and, thus, it is a good approximation to replace the curly braces in Eq. (C15) by unity. Recalling the definition (C3) of F(E) and then using the relation (C12), we obtain

$$G_{2}(T_{1}, T_{e}; E_{0}) \simeq \frac{1}{E_{0} \mathcal{A}(E_{0})} \int_{E_{0}}^{\infty} dE \left\{ E \frac{\mathcal{A}_{I}(E) \mathcal{A}_{e}(E)}{\langle T \mathcal{A}(E) \rangle} \right\} \exp\{-[S(E) - S(E_{0})]\}$$

$$= -\frac{1}{E_{0} \mathcal{A}(E_{0})} \int_{E_{0}}^{\infty} dE E \frac{\mathcal{A}_{I}(E) \mathcal{A}_{e}(E)}{\mathcal{A}(E)} \frac{d}{dE} \exp\{-[S(E) - S(E_{0})]\}$$

$$= \frac{\mathcal{A}_{I}(E_{0}) \mathcal{A}_{e}(E_{0})}{\mathcal{A}^{2}(E_{0})} + \frac{1}{E_{0} \mathcal{A}(E_{0})} \int_{E_{0}}^{\infty} dE \exp\{-[S(E) - S(E_{0})]\} \frac{d}{dE} \left[E \frac{\mathcal{A}_{I}(E) \mathcal{A}_{e}(E)}{\mathcal{A}(E)} \right]. \tag{C17}$$

As before, we have the estimate

$$\frac{d}{dE} \left[E \frac{\mathcal{A}_{\mathsf{I}}(E)\mathcal{A}_{e}(E)}{\mathcal{A}(E)} \right] \sim \frac{\mathcal{A}_{\mathsf{I}}(E)\mathcal{A}_{e}(E)}{\mathcal{A}(E)} = \frac{\langle T\mathcal{A}(E)\rangle}{E \mathcal{A}(E)} \left[E \frac{\mathcal{A}_{\mathsf{I}}(E)\mathcal{A}_{e}(E)}{\langle T\mathcal{A}(E)\rangle} \right] \sim \frac{T}{E} \left[E \frac{\mathcal{A}_{\mathsf{I}}(E)\mathcal{A}_{e}(E)}{\langle T\mathcal{A}(E)\rangle} \right]. \tag{C18}$$

Here again T represents a typical plasma temperature, and since the integration region starts at $E = E_0$, we have $T/E \le T/E_0$. Since the factor in the square brackets in the last line in Eq. (C18) is just the factor in the curly braces in the first line in Eq. (C17), we see that the last line in Eq. (C17) is of order T/E_0 times the first line and, thus, gives a correction on the order of a few

percentages. We have found that, to within corrections of a few percentages,

$$G_2(T_1, T_e; E_0) \simeq \frac{\mathcal{A}_1(E_0) \,\mathcal{A}_e(E_0)}{\mathcal{A}^2(E_0)}.$$
 (C19)

The accuracy of the analytical approximation (C19) for G_2 has been confirmed to this precision by direct numerical evaluation of its definition (C6).

In summary, Eq. (C4) expresses the G function in three parts. The first part G_1 involves a triple integral that must be evaluated by numerical computation. This evaluation is simplified because, with the partition that we have made, the regions of integration that appear in G_1 are restricted to the finite interval $0 < E < E_0$. For the second part G_2 , the approximation (C19) is sufficiently accurate for our purposes. The remainder G_3 is very small and we may simply set

$$G_3(T_1, T_e; E_0) = 0.$$
 (C20)

^[1] R. L. Singleton Jr. and L. S. Brown, Plasma Phys. Contr. F. 50, 124016 (2008).

^[2] L. S. Brown, D. L. Preston, and R. L. Singleton Jr., Phys. Rev. E 86, 016406 (2012).

^[3] L. S. Brown, D. L. Preston, and R. L. Singleton Jr., Phys. Rep. 410, 237 (2005).

^[4] L. S. Brown and R. L. Singleton Jr., Phys. Rev. E 76, 066404 (2007).

^[5] G. Dimonte and J. Daligault, Phys. Rev. Lett. 101, 135001 (2008).

^[6] J. D. Huba, *NRL Plasma Formulary* (Naval Research Lab., Washington, DC, 2004).